RESEARCH ARTICLE

Integrating Contact, Modeling, and Control for the Robotic Hand Manipulation

SHUWEI ZHAO[1], JIN YU[2], YE-HWA CHEN[3], AND RUIYING ZHAO[1], (Member, IEEE)

[1]National Engineering Research Center of Highway Maintenance Equipment, Chang'an University, Xi'an 710065, China
[2]School of Automation, Beijing Institute of Technology, Beijing 100081, China
[3]The George W. Woodruff School of Mechanical Engineering, Georgia Institute of Technology, Atlanta, GA 30332, USA

Corresponding author: Ruiying Zhao (ruiying.zhao@chd.edu.cn)

ABSTRACT A novel manipulation control framework is proposed for the dexterous robotic hand, which integrates the constraints (contact constraints and servo constraints), dynamics modeling and controller design. In the manipulation task, the contact between the robotic hand and the target object translates the manipulating force and constraints the relative motion of the target. Hence, the contact forces can be considered as the bridge for the robotic hand manipulation and the motion control of the target object. By the Udwadia-Kalaba theory, the dynamics model of the contact forces for the rolling manipulation in the work space is constructed explicitly without any auxiliary variable and calculated by the states of the robotic hand (such as, the angular and velocity of the finger joints) and the local variables of the target object (e.g., the surface parameters). Based on the formulated contact forces, an integrated control strategy is introduced to tackle with the manipulation task by combining the desired motion of the target object and the manipulation controller design through the contact constraints. Virtue of the calculated contact forces, the proposed control could accomplish the manipulation tasks without force sensors. Besides, to ensure the trajectory of the object is smooth and continuous, a grasping plan for the dexterous robotic hand is proposed. The effectiveness of the control is verified by both theoretical proof and the numerical simulation of a three fingered robotic hand in 3D workspace.

I. INTRODUCTION

As a kind of flexible end-effector mechanism with a high degree of freedom, a dexterous robotic hand could accomplish various complex and precise tasks. It has a wide range of applications, such as industrial manufacturing [1], [2], domestic service [3], [4], space exploration [5], medical rehabilitation [6], [7], and dangerous goods handling [8]. Those tasks can be divided into two groups: "grasping" and "manipulation". The former one requires fingers (might include palm) to meet the form or force closure with the target object to ensure stable grasping. The latter one

The associate editor coordinating the review of this manuscript and approving it for publication was Guilin Yang.

manipulates the object by moving the fingers joints, which is based on the grasp of the object. In comparison to the conventional grasping tasks, the robotic hand manipulation covers a broader range of contact types, and each of these distinct contact types exerts different effects on the object manipulation task (the variation in contact forces applied by the hand to the object, intuitively). Furthermore, the differing contact forces increase the difficulty of the manipulation control design. Hence, how to realize the highly precise dynamic manipulation control of the dexterous robotic hand under differing contact types becomes the focus.

Since the manipulation of the robotic hand relies significantly on the contact forces, the manipulation control design in previous research works can be divided into two

groups: contact forces estimation-based controls and contact forces model-based controls. For those controls without the use of analytical contact forces model, [9], [10] proposes a series of empirical control approaches. In [9], the contact forces can be estimated based on the detection model, which is built by a deep neural network from the tactile data of the objects collected by the tactile sensor. The controller utilizes the estimated contact forces to empower the robotic hand in manipulating the target object, even in the absence of prior knowledge about the object's shape or physical characteristics. Reference [10] employs an recurrent neural network with a parametric bias to forecast the contact state, thereby achieving hand robot contact control by aligning current contact forces with the desired target values. The above control approaches, which rely entirely on artificial intelligence-related technologies, are easily applied and can estimate the contact forces with no need for an analytical model of the hand robot. Nevertheless, achieving optimal performance with such controllers heavily relies on the quality of the collected data, necessitating a substantial investment of time and resources in training with a significant amount of data. Besides, [11], [12] introduce several controllers to accomplish the manipulation tasks by using the model of the hand robot. Reference [11] presents a approach for in-hand manipulation based on the inverse kinematic model of the robotic hand, which able to change the location of the object by the hand robot based on rolling contact model. Reference [12] employs an in-hand manipulation controller to attain the intended sliding motion amidst a cluster of grapes, relying on a model that characterizes the dynamics of the sliding process. It predicts the sliding directions by the contact pressure distribution at each finger, effectively mitigating errors resulting from trajectory tracking inaccuracies. The control method proposed in [13] utilizes the dynamic model of the robotic hand, which can detect slippage between fingers and the target object using a force sensor. By this controller, it successes to adjust the contact forces to a proper value for the object manipulation. Such control designs introduced above can get the contact forces directed by the force sensor. It is very simple but has no knowledge about the relationship between the contact force and the finger joint variables, which means it will be a little difficult for contact forces controlling in a high precision.

For those contact forces model-based controls, several methods developed in [14] and [15]. Reference [14] combines the dynamic models of the dexterous robotic hand and the target object, which aims to calculate the fingertip contact forces. It introduces a controller based on the contact forces to manipulate the object tracking the desired trajectory with no slipping contact. Same as [14] and [15] formulates the contact forces using the combined dynamic model. It analysis the influence of the object's gravity on the contact forces and calculates the relationship between these forces and the fingers joints driving torques. The controller designed in [16], which is based on the contact constrained forces using Lagrange multipliers, can make

sure the object will be continuously moving within the hand without dropping. Those control methods mentioned above establish the dynamic model of the hand in contact with the object by building the dynamic model of the hand and the object separately at first. Then, by combining those two models, the contact forces can be conducted. However, those controllers designed based on the contact forces model are always not considering the coupling issue between the fingertip contact forces and the joint driving torques, which will influence the accuracy of the manipulation. Reference [17] addresses the coupling issue in the context of a dexterous robotic hand interacting with a target object. The approach treats the robotic hand and the target object as a unified system. This system's dynamic model is established using the Udwadia-Kalaba equation, enabling the explicit derivation of fingertip contact forces within the workspace. Importantly, this method decouples these contact forces from the control torques applied to the finger joints. Consequently, the dynamic control approach proposed in [17] can guide the target object along a desired trajectory without the need for force sensors. For the more sophisticated manipulation, it is natural to take the manipulation system's uncertainty into consideration, [18], [19], [20] demonstrate some promising strategy in complex dynamic system's uncertainty modeling and control designing.

The study we did previously in [17] discusses the dynamic control design when the dexterous robotic hand is in fixed contact with the target object. However, the non-fixed contacts also can be found in those manipulation tasks that aim to adjust the position of the target object [21]. The most common non-fixed contacts involve pure rolling contact, twist rolling contact, and slide rolling contact. When the robotic hand is in slide rolling contact with the object, there will be the relative velocity at the contact point, which may impact the accuracy of the object manipulation. Hence, slide rolling contact is always needing to be avoided during the manipulation. The kinematic analysis of the twist rolling contact between a robotic hand and an object can be simplified by considering it as a form of pure rolling contact. Therefore, we consider discussing the dynamic control design method of the dexterous robotic hand manipulation system with pure rolling contact constraints.

The hand-object manipulation system's inertia matrix is singular caused by the pure rolling constraints. Therefore, to formulate the system dynamic model, the extended Udwadia-Kalaba equation mentioned in [22] is used in this paper. Based on the fingertip contact force model derived from the dynamic model of the system, we attempt to design the control by the constraint-following control method. This control method discussed in [23] and [24] treats the control target as servo constraints and proposes the control using the servo constrained forces, which can be conducted by the extended Udwadia-Kalaba equation.

There are four contributions in this paper. First, the kinematic model of the dexterous robotic hand and contact constraints in the pure rolling contact are build. Second, the

necessary condition for a stable grasp planning is analyzed to guarantee the object's trajectory smooth and continuous. Third, based on the derived contact constraints, the analytical contact forces model in the manipulation workspace is constructed by the extended Udwadia Kalaba equation without any auxiliary variable. Fourth, the manipulation task is transformed into a constraint-following problem. After decoupling the contact forces with the finger joint torques, a contact forces model-based dynamic control of the dexterous robotic hand manipulation system is established. The theoretical analysis guaranteed the proposed control strategy's effectiveness, and the further simulation results demonstrate that the dexterous robotic hand can perform the precise manipulation control without any force sensors.

The remainder of this paper is organized as follows. Section II presents the foundational mathematical concepts used in the paper. Section III develops the kinematic model of the dexterous robotic hand operating under the pure rolling contact constraints. In Section IV, the condition of the grasp planning for the stable manipulation is discussed. An analytical model of the contact forces in the manipulation workspace is constructed in Section V. Section VI focuses on the establishment of the contact force model-based dynamic control system for the dexterous robotic hand manipulation. Section VII provides the detailed simulations of a three-fingered dexterous robotic hand and verifies the effectiveness of the proposed control. Finally, the paper concludes a summary in the last section.

II. RELATED MATHEMATICAL FOUNDATIONS
A. UDWADIA-KALABA THEORY
In a mechanical system consists of particles and rigid bodies, the system's configuration can be described by a set of generalized coordinate $\theta \in R^n$. The corresponding generalized velocity and acceleration are denoted by $\dot{\theta} \in R^n$ and $\ddot{\theta} \in R^n$. By employing Lagrange equation, the unconstrained dynamic model of the system can be represented as

$$M(\theta, t)\ddot{\theta} = F(\theta, \dot{\theta}, t), \qquad (1)$$

where $M(\theta, t) = M^T(\theta, t) \in R^{n \times n}$ is the inertia matrix and $F(\theta, \dot{\theta}, t) \in R^n$ encompasses various effects include contributions from gravitational force, externally applied forces, as well as Coriolis and centrifugal forces due to the system's motion.

Assume that the system is subject to l Pfaffian, where $l < n$, these constraints can be either holonomic or non-holonomic in nature

$$\sum_{s=1}^{n} Q_{rs}(\theta, t)\dot{\theta}_s + c_r(\theta, t) = 0 \quad (r = 1, 2, \ldots, l), \qquad (2)$$

where $Q_{rs}(\cdot): R^n \times R \to R$ and $c_r(\cdot): R^n \times R \to R$ are both C^1. The l constraints can be consolidated and depicted in a concise matrix form as

$$Q(\theta, t)\dot{\theta} + c(\theta, t) = 0, \qquad (3)$$

where $Q(\theta, t) \in R^{l \times n}$ and $c(\theta, t) \in R^l$. Differentiating (3) with respect to t yields

$$Q(\theta, t)\ddot{\theta} = -\dot{c}(\theta, t) - \dot{Q}(\theta, t)\dot{\theta} =: b(\theta, \dot{\theta}, t). \qquad (4)$$

According to [22], there will be

$$\begin{bmatrix} \left(I - Q^+(\theta, t)Q(\theta, t)\right) M(\theta, t) \\ Q(\theta, t) \end{bmatrix} \ddot{\theta}$$
$$= \begin{bmatrix} \left(I - Q^+(\theta, t)Q(\theta, t)\right) \left(F(\theta, \dot{\theta}, t) + C(\theta, \dot{\theta}, t)\right) \\ b(\theta, \dot{\theta}, t) \end{bmatrix}, \qquad (5)$$

where $C(\dot{\theta}, \theta, t)$ represents an n-dimensional vector that describes the properties of non-ideal constraints, which can be identified according to [25].

Assumption 1: For matrix $\begin{bmatrix} \left(I - Q^+(\theta, t)Q(\theta, t)\right) M(\theta, t) \\ Q(\theta, t) \end{bmatrix} \in R^{(n+l) \times n}$, the matrix's rank will be equal to n.

Assumption 2: The equation (5) is consistent, indicating that there always exists at least one solution $\ddot{\theta}$ to equation (5).

Theorem 1: Subject to Assumptions 1-2, the dynamic model of the mechanical system (1) which is subject to constraints (4) can be expressed as [22]

$$\ddot{\theta} = \begin{bmatrix} \left(I - Q^+(\theta, t)Q(\theta, t)\right) M(\theta, t) \\ Q(\theta, t) \end{bmatrix}^+$$
$$\begin{bmatrix} \left(I - Q^+(\theta, t)Q(\theta, t)\right) \left(F(\theta, \dot{\theta}, t) + C(\theta, \dot{\theta}, t)\right) \\ b(\theta, \dot{\theta}, t) \end{bmatrix}. \qquad (6)$$

The extended Udwadia-Kalaba equation remains applicable to the constrained mechanical systems, irrespective of the inertia matrix's rank. Therefore, it can handle situations where the inertia matrices are singular, without imposing any restrictions. The constrained force $F^c(\theta, \dot{\theta}, t)$ can be represented according to the dynamic model (5) as

$$F^c(\theta, \dot{\theta}, t)$$
$$= M(\theta, t) \begin{bmatrix} \left(I - Q^+(\theta, t)Q(\theta, t)\right) M(\theta, t) \\ Q(\theta, t) \end{bmatrix}^+$$
$$\begin{bmatrix} \left(I - Q^+(\theta, t)Q(\theta, t)\right) \left(F(\theta, \dot{\theta}, t) + C(\theta, \dot{\theta}, t)\right) \\ b(\theta, \dot{\theta}, t) \end{bmatrix}$$
$$- \left(F(\theta, \dot{\theta}, t) + C(\theta, \dot{\theta}, t)\right). \qquad (7)$$

The constrained force, obtained by the extended Udwadia-Kalaba equation, is expressed in an analytic form, and notably, it does not involve any auxiliary variables. When the inertia matrix $M(\theta, t)$ in (7) to be non-singular, the constrained force $F^c(\theta, \dot{\theta}, t)$ can be simplified as the one obtained by the Udwadia-Kalaba equation in [26].(The proof can be seen in [22]).

B. RELATED LEMMA
To express the contact forces between the dexterous robotic hand and the target object, those Lemmas needed are introduced here.

Lemma 1: For the matrix $\begin{bmatrix} (I - Q^+(\theta, t)Q(\theta, t))M(\theta, t) \\ Q(\theta, t) \end{bmatrix}$ $\in R^{(n+l) \times n}$, if the rank of this matrix is n, there will be $Rank\left(\begin{bmatrix} M(\theta, t) \\ Q(\theta, t) \end{bmatrix}\right) = n$ and vice versa [22].

The Lemma 1 introduced above is related to the extended Udwadia-Kalaba equation. $M(\theta, t)$ and $Q(\theta, t)$ have the same meaning as those two in Theorem 1.

Lemma 2: For any matrix $W \in R^{n \times m}$ (m < n) which satisfies Rank(W)=m(m $\geq$ 1), then there will be [27]

$$W^+ = (W^T W)^{-1} W^T. \tag{8}$$

Lemma 3: For given matrices $S \in R^{n \times m}$ and $H \in R^{m \times k}$, if Rank(S)=r and Rank(H)=l (r,l $\geq$ 1), there will be [28]

$$(SH)^+ = H^+(S^+ SHH^+)^+ S^+. \tag{9}$$

Lemma 4: Consider a matrix $G \in R^{n \times m}$ which with rank r (r $\geq$ 1), there will be [29]

$$(G^+ G)^+ = G^+ G, \tag{10}$$

$$G^+ G G^+ = G^+. \tag{11}$$

Lemma 5: Consider a non-singular matrix $\tilde{E} \in R^{n \times n}$, a matrix $\tilde{J} \in R^{n \times m}$, a non-singular matrix $\tilde{O} \in R^{m \times m}$, and a matrix $\tilde{K} \in R^{m \times n}$, there will be [30]

$$\begin{aligned} (\tilde{E} + \tilde{J}\tilde{O}\tilde{K})^{-1} &= \tilde{E}^{-1} - \tilde{E}^{-1}\tilde{J}(I + \tilde{O}\tilde{K}\tilde{E}^{-1}\tilde{J})^{-1}\tilde{O}\tilde{K}\tilde{E}^{-1} \\ &= \tilde{E}^{-1} - \tilde{E}^{-1}\tilde{J}\tilde{O}\tilde{K}(I + \tilde{E}^{-1}\tilde{J}\tilde{O}\tilde{K})^{-1}\tilde{E}^{-1} \\ &= \tilde{E}^{-1} - \tilde{E}^{-1}\tilde{J}(\tilde{O}^{-1} + \tilde{K}\tilde{E}^{-1}\tilde{J})^{-1}\tilde{K}\tilde{E}^{-1}, \end{aligned} \tag{12}$$

since

$$\begin{aligned} |I + \tilde{O}\tilde{K}\tilde{E}^{-1}\tilde{J}| &= |\tilde{O}^{-1} + \tilde{K}\tilde{E}^{-1}\tilde{J}||\tilde{O}| \\ &= |I + \tilde{E}^{-1}\tilde{J}\tilde{O}\tilde{K}| \\ &= |\tilde{E}^{-1}||\tilde{E} + \tilde{J}\tilde{O}\tilde{K}| \neq 0. \end{aligned} \tag{13}$$

Therefore, $(\tilde{O}^{-1} + \tilde{K}\tilde{E}^{-1}\tilde{J})^{-1}$ will exist.

Lemma 6: Consider a matrix $P \in S^{n \times n}$ which makes $(I + S)$ non-singular, there will be [30]

$$(I + S)^{-1} = I - (I + S)^{-1}P, \tag{14}$$

$$(I + S)^{-1} = I - S(I + S)^{-1}. \tag{15}$$

III. THE KINEMATICS OF THE DEXTEROUS ROBOTIC HAND WITH PURE ROLLING CONTACTS

Consider the scenario where a dexterous robotic hand interacts with an object (Fig. 1). The robotic hand consists of three identical fingers, all sharing the same structure with a distal phalanx, middle phalanx, and proximal phalanx (shown in Fig. 2). The robotic hand has three joints on each of its fingers, all of which are actuated by servo motors. Moreover, each finger possesses four degrees of freedom: the first joint, connected to the palm base, has two degrees of freedom, while the second and third joints each have one degree of freedom.
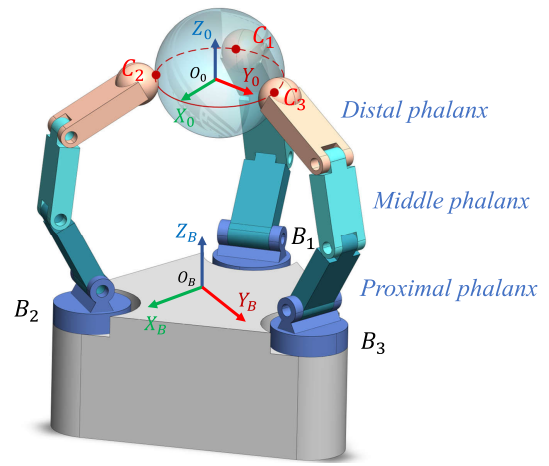

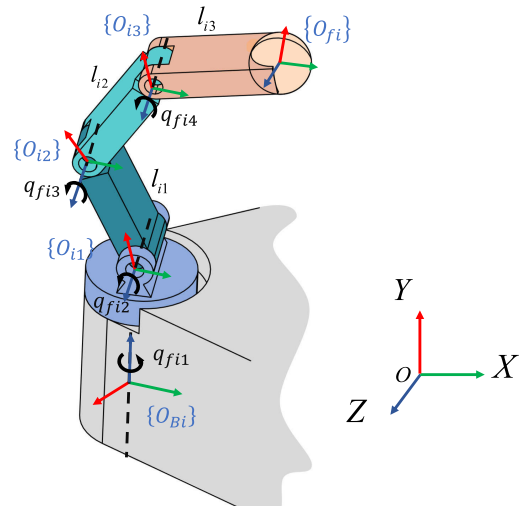**FIGURE 1.** Three-fingered robotic hand in contact with an object.

FIGURE 2. The ith finger(i = 1, 2, 3).

Let $\{O_B\}$ and $\{O_{Bi}\}$ be the primary coordinate frame of the robotic hand and the ith finger primary coordinate frame, without a relative rotation relationship between those two. Set $\{O_{i(j-1)}\}$ to be the coordinate frame fixed in the jth knuckle and $\{O_{i0}\}$ is overlapped with $\{O_{Bi}\}$. Set $\{O_{fi}\}$ to be the fixed coordinate frame in the mass center of the ith fingertip. Lastly, let $\{O_o\}$ denote the coordinate frame located at the object's mass center. The parameters of the ith finger are defined as following:

q_{fi_j} - the jth rotation angle (j = 1, 2, 3, 4.);
l_{ik} - the length of the kth phalanx (k = 1, 2, 3.);
m_{ik} - the mass of the kth phalanx;
I_{ik} - the inertia moment of the kth phalanx.

To depict the contact points' location on the fingertips and the surface of the object, we establish the mappings: $^{fi}C_{fi}(\cdot) : R^2 \to R^3$ and $^oC_{oi}(\cdot) : R^2 \to R^3$. Suppose α_{fi}, $\alpha_{oi} \in R^2$ are local parameters of the ith fingertip surface and the object surface. Then, $^{fi}C_{fi}(\alpha_{fi})$ is a point on the surface of

the ith fingertip in $\{O_{fi}\}$ coordinate frame, and $^oC_{oi}(\alpha_{oi})$ is a point on the of object surface in $\{O_o\}$ coordinate frame.

Choose $q_{fi} = [q_{fi_1}, q_{fi_2}, q_{fi_3}, q_{fi_4}, \alpha_{fi}]^T$ and $q_{oi} = [x_o, y_o, z_o, \phi_o, \theta_o, \psi_o, \alpha_{oi}]^T$ as the generalized coordinates of the ith finger and the target object, where, $\{x_o, y_o, z_o\}$ and $\{\phi_o, \theta_o, \psi_o\}$ are the positions and the Euler angles of the object. Then, the positions of the ith fingertip surface contact-point P_{fci} and the object surface contact-point P_{oci} in the primary coordinate frame $\{O_B\}$ can be presented as [31]

$$P_{fci}(q_{fi}) = P_{fi}(q_{fi}) + R_{fi}(q_{fi})^{fi}C_{fi}(\alpha_{fi}), \quad (16)$$

$$P_{oci}(q_{oi}) = P_o(q_{oi}) + R_o(q_{oi})^oC_{oi}(\alpha_{oi})), \quad (17)$$

where $P_{fi}(q_{fi}) \in R^3$ is the position vector of mass center of the ith fingertip, and $P_o(q_{oi}) \in R^3$ is the position vector of the object mass center in the primary coordinate frame $\{O_B\}$. $R_{fi}(q_{fi}) \in R^{3\times3}$ is the rotation matrix of the coordinate frame $\{O_{fi}\}$ relative to the primary coordinate frame $\{O_B\}$, and $R_o(q_{oi}) \in R^{3\times3}$ is the rotation matrix of the coordinate frame $\{O_o\}$ relative to the primary coordinate frame $\{O_B\}$.

In order to interact with the object, the robotic hand must establish point contact with the object using its multiple fingers, as discussed in this paper. Suppose i^{th} fingertip and object in contact at time t and set the contact points are $P_{fci}(q_{fi})$ and $P_{oci}(q_{oi})$, the positions of those two contact points will always equal to each other as

$$P_{fi}(q_{fi}) + R_{fi}(q_{fi})^{fi}C_{fi}(\alpha_{fi}) = P_o(q_{oi}) + R_o(q_{oi})^oC_{oi}(\alpha_{oi}). \quad (18)$$

When the tip of the finger is in a state of pure rolling contact with the target object., there will be relative moving between the contact point and the surface it is located. However, there is no relative velocity between those two contact points, which means

$$R_{fi}(q_{fi})^{fi}\dot{C}_{fi}(\alpha_{fi}, \dot{\alpha}_{fi}) = R_o(q_{oi})^o\dot{C}_{oi}(\alpha_{oi}, \dot{\alpha}_{oi}). \quad (19)$$

Besides, suppose the fingertips have continuous contact with the target object, which means the fingertips and the object will not separate or penetrate at the contact points. The contact considered in this paper is a rigid contact between the hemispherical fingertips and the spherical object. Hence, the relationship between those two outward unit normal vectors at the contact points should be

$$R_{fi}(q_{fi})^{fi}e_{fi}(\alpha_{fi}) = -R_o(q_{oi})^oe_{oi}(\alpha_{oi}), \quad (20)$$

where $^{fi}e_{fi}(\alpha_{fi})$ denotes the outward unit normal vector of the contact point $P_{fci}(q_{fi}, \alpha_{fi})$ in coordinate frame $\{O_{fi}\}$, $^oe_{oi}(\alpha_{oi})$ denotes the outward unit normal vector of the contact point $P_{oci}(q_{oi}, \alpha_{oi})$ in coordinate frame $\{O_o\}$.

Take the derivative of (18) yields

$$\dot{P}_{fi}(q_{fi}, \dot{q}_{fi}) + \dot{R}_{fi}(q_{fi}, \dot{q}_{fi})^{fi}C_{fi}(\alpha_{fi})$$
$$+ R_{fi}(q_{fi})^{fi}\dot{C}_{fi}(\alpha_{fi}, \dot{\alpha}_{fi})$$
$$= \dot{P}_o(q_{oi}, \dot{q}_{oi}) + \dot{R}_o(q_{oi}, \dot{q}_{oi})^oC_{oi}(\alpha_{oi}) + R_o(q_{oi})^o\dot{C}_{oi}(\alpha_{oi}, \dot{\alpha}_{oi}), \quad (21)$$

Differentiating (20) to get

$$(\omega_{fi}\times)R_{fi}(q_{fi})^{fi}e_{fi}(\alpha_{fi}) + R_{fi}(q_{fi})^{fi}\dot{e}_{fi}(\alpha_{fi}, \dot{\alpha}_{fi})$$
$$+ (\omega_{oi}\times)R_o(q_{oi})^oe_{oi}(\alpha_{oi}) + R_o(q_{oi})^o\dot{e}_{oi}(\alpha_{oi}, \dot{\alpha}_{oi}) = 0. \quad (22)$$

Here, $\omega_{fi} = [\omega_{fi1}, \omega_{fi2}, \omega_{fi3}]^T$ and $\omega_{oi} = [\omega_{o1}, \omega_{o2}, \omega_{o3}]^T$ are the angular velocity of the $\{O_{fi}\}$ and $\{O_o\}$, respectively.

Combining (21), (19), and (22), the pure rolling contact constraints using the coordinates q_{fi} and q_{oi} can be represented in a matrix form as

$$\begin{bmatrix} A_{fi} & A_{oi} \end{bmatrix} \begin{bmatrix} \dot{q}_{fi} \\ \dot{q}_{oi} \end{bmatrix} = 0, \quad (23)$$

where $A_{fi} = \begin{bmatrix} D_{fi}J_{fi} & 0_{3\times2} \\ 0_{3\times4} & R_{fi}(\partial^{fi}C_{fi}/\partial\alpha_{fi}) \\ E_{fi}J_{fi} & R_{fi}(\partial^{fi}e_{fi}/\partial\alpha_{fi}) \end{bmatrix}$ and $A_{oi} = \begin{bmatrix} D_{oi} & 0_{3\times2} \\ 0_{3\times6} & -R_o(\partial^oC_{oi}/\partial\alpha_{oi}) \\ E_{oi} & R_o(\partial^oe_{oi}/\partial\alpha_{oi}) \end{bmatrix}$. Here, $D_{fi} := \begin{bmatrix} I_{3\times3} & -(R_{fi}^{fi}C_{fi}\times) \end{bmatrix}$, $E_{fi} := \begin{bmatrix} 0_{3\times3} & -(R_{fi}^{fi}e_{fi}\times) \end{bmatrix}$, $D_{oi} := \begin{bmatrix} -I_{3\times3} & (R_o^oC_{oi}\times) \end{bmatrix}$, and $E_{oi} := \begin{bmatrix} 0_{3\times3} & -(R_o^oe_{oi}\times) \end{bmatrix}$. J_{fi} is the Jacobian matrix mapping of the ith finger motion from the joint to the fingertip.

When the ith finger in pure rolling contact with the object, there will be two holonomic constraints in (18) and (20) and one non-holonomic constraint in (19). Due to the surface mapping function $^{fi}C_{fi}(\cdot)$ and $^oC_{oi}(\cdot)$, the contact positions in R^3 can be expressed by α_{fi} and α_{oi} in R^2, which means (18) will limit two degrees of freedom with three equations. Similarly, the unit normal vector in R^3 can be calculated with two parameters, and (21) will only reduce two degrees of freedom of the kinematics. Hence, there will be two degrees of freedom for the relative motion when the ith finger is in pure rolling contact with the object.

IV. GRASP PLANNING FOR THE DEXTEROUS ROBOTIC HAND

During the manipulation process, the target object will be driven to its desired trajectory by the robotic hand. If the trajectory of the object is not smooth, it may result in the discontinuous velocity of the object and the failed dynamic manipulation. Consequently, it becomes imperative to develop a stable grasp planning strategy to ensure a continuous and smooth trajectory for the object. This, in turn, serves as a prerequisite for the subsequent dynamic manipulation control.

To ensure the moving trajectory is continuous and smooth, the force relationship between fingertips and the object needs to be analyzed first. Let $f_{ci} \in R^3$ and $n_{ci} \in R^3$ to be the force and torque act on the contact point C_i in the primary coordinate frame. $f_o \in R^3$ and $n_o \in R^3$ are the force and torque in the mass center of the target object in the primary coordinate frame. Then, the force relationship between the three-fingered robotic hand and the object shown in Fig. 3
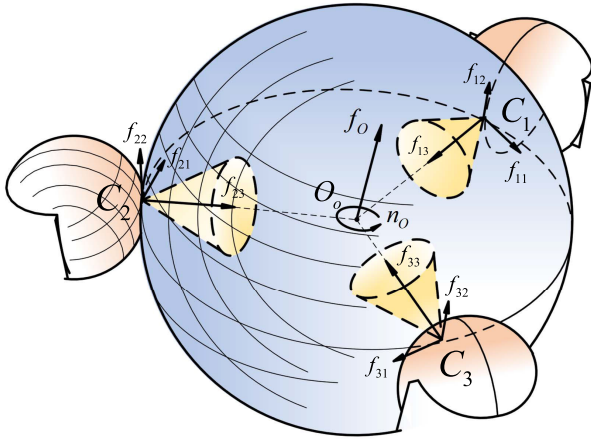
FIGURE 3. The force relationship between the three-fingered robotic hand and the object.

can be formulated as

$$F_o := \begin{bmatrix} f_o \\ n_o \end{bmatrix} = \sum_{i=1}^{3} \begin{bmatrix} I_{3\times3} & 0_{3\times3} \\ R_o^o C_{oi} \times & I_{3\times3} \end{bmatrix} \begin{bmatrix} f_{ci} \\ n_{ci} \end{bmatrix} =: \sum_{i=1}^{3} W_{oci} F_{ci}. \tag{24}$$

According to the pure rolling contact model at the contact point C_i showed in Fig. 3, the friction cones is given by

$$FC_i = [f_i = (f_{i1}, f_{i2}, f_{i3}, f_{i4})^T : \sqrt{f_{i1}^2 + f_{i2}^2} \le \mu f_{i3},$$
$$f_{i3} \ge 0, |f_{i4}| \le \bar{\gamma} f_{i3}], \tag{25}$$

where μ and $\bar{\gamma}$ are the static friction coefficient and the torsional friction coefficient, which are both always greater than zero, and f_i is the force expressed in the fixed frame $\{O_{Ci}\}$ at the contact point C_i. The relationship between the f_i and F_{ci} can be given by

$$F_{ci} = \begin{bmatrix} R_{ci} \\ & R_{ci} \end{bmatrix} \begin{bmatrix} I_{3\times3} & 0_{3\times1} \\ 0_{3\times3} & z_{bi} \end{bmatrix} f_i =: H_{ci} f_i, \tag{26}$$

where $z_{bi} = [0, 0, 1]^T$ and $R_{ci} \in R^{3\times3}$ is the rotation matrix of the frame $\{O_{Ci}\}$ relative to the primary frame $\{O_B\}$. Substituting (26) into (24) yields

$$F_o = \sum_{i=1}^{3} W_{oci} H_{ci} f_i =: \sum_{i=1}^{3} G_{Ci} f_i, \tag{27}$$

where $G_{Ci} \in R^{6\times4}$ is a mapping of the object motion from the surface to the mass center of the object.

According to the constraints analyzed in (19), the velocities of contact points in the object and the fingertip surface will equal each other. Hence, this relationship can be displayed under the coordinate frame $\{O_{Ci}\}$ as

$$H_{ci}^T \left(\begin{bmatrix} \dot{P}_{fci} \\ \omega_{fci} \end{bmatrix} - \begin{bmatrix} \dot{P}_{oci} \\ \omega_{oci} \end{bmatrix} \right) = 0. \tag{28}$$

Differentiating (16) and (17), there will be

$$\begin{bmatrix} \dot{P}_{fci} \\ \omega_{fci} \end{bmatrix} = \begin{bmatrix} I_{3\times3} & -(R_{fi}^{fi} C_{fi} \times) & R_{fi}(\partial^{fi} C_{fi}/\partial \alpha_{fi}) \\ 0_{3\times3} & I_{3\times3} & 0_{3\times2} \end{bmatrix} \begin{bmatrix} \dot{P}_{fi} \\ \omega_{fi} \\ \alpha_{fi} \end{bmatrix}$$
$$=: W_{fci}^T \begin{bmatrix} \dot{P}_{fi} \\ \omega_{fi} \\ \alpha_{fi} \end{bmatrix}, \tag{29}$$

and

$$\begin{bmatrix} \dot{P}_{oci} \\ \omega_{oci} \end{bmatrix} = \begin{bmatrix} I_{3\times3} & -(R_o^o C_{oi} \times) & R_o(\partial^o C_{oi}/\partial \alpha_{oi}) \\ 0_{3\times3} & I_{3\times3} & 0_{3\times2} \end{bmatrix} \begin{bmatrix} \dot{P}_o \\ \omega_o \\ \alpha_{oi} \end{bmatrix}$$
$$=: W_{oci}^T \begin{bmatrix} \dot{P}_o \\ \omega_o \\ \alpha_{oi} \end{bmatrix}. \tag{30}$$

Substituting (29) and (30) into (28) yields

$$G_C^T \begin{bmatrix} \dot{P}_o \\ \omega_o \end{bmatrix} = \begin{bmatrix} J_{c1} & & \\ & J_{c2} & \\ & & J_{c3} \end{bmatrix} \begin{bmatrix} \dot{q}_{f1} \\ \dot{q}_{f2} \\ \dot{q}_{f3} \end{bmatrix} - \begin{bmatrix} hr_1 & & \\ & hr_2 & \\ & & hr_3 \end{bmatrix} \begin{bmatrix} \alpha_{o1} \\ \alpha_{o2} \\ \alpha_{o3} \end{bmatrix}$$
$$=: J_c \dot{q}_f - H_r \alpha_o, \tag{31}$$

where $hr_i = \begin{bmatrix} R_{ci}^T R_o(\partial^o C_{oi}/\partial \alpha_{oi}) \\ 0_{1\times2} \end{bmatrix} \in R^{4\times2}$, $J_{ci} = H_{ci}^T W_{fci}^T \hat{J}_{fi} \in R^{4\times6}$, $\hat{J}_{fi} = \begin{bmatrix} J_{fi} & 0_{6\times2} \\ 0_{2\times4} & 0_{2\times2} \end{bmatrix} \in R^{8\times6}$, and $G_C = [G_{C_1}, G_{C_2}, G_{C_3}]$.

Assumption 3: Equation (31) is consistent: for any G_C^T and $(J_c \dot{q}_f - H_r \alpha_o)$, there exists at least one solution $[\dot{P}_o^T, \omega_o^T]^T$ to (31).

Remark 1: According to Assumption 3, there will be

$$G_C^T (G_C^T)^+ (J_c \dot{q}_f - H_r \alpha_o) = J_c \dot{q}_f - H_r \alpha_o. \tag{32}$$

Suppose the Assumption 3 is satisfied, the velocity of the object can be given by

$$[\dot{P}_o^T, \omega_o^T]^T = (G_C^T)^+ (J_c \dot{q}_f - H_r \alpha_o) + (I - (G_C^T)^+ G_C^T)\eta. \tag{33}$$

where any vector $\eta \in R^6$. This vector will not be influenced by the joint velocity of the hand robot, which means it is a parameter that can not be controlled by the input torques.

Assumption 4: For the grasp matrix G_C, there will be Rank(G_C)=6.

Remark 2: When the grasp matrix G_C has full row rank, G_C^T will be a column non-singular matrix. According to lemma 2, there will be $(G_C^T)^+ = (G_C G_C^T)^{-1} G_C$, so that $(I - (G_C^T)^+ G_C^T)\eta$ in (33) can be solved.

Theorem 2: If the hand robot manipulates an object under the pure rolling contact and subjects to Assumptions 3-4, the trajectory of the target object will be smooth and continuous.

Proof of Theorem 2: When the hand robot manipulation system subject to Assumption 3-4, the target object's velocity can be expressed as (33) and there will be

$(G_C^T)^+ = (G_C G_C^T)^{-1} G_C$ leading to $(I - (G_C^T)^+ G_C^T) = 0$. Hence, the velocity of the object can be rewritten as

$$[\dot{P}_o^T, \omega_o^T]^T = (G_C^T)^+(J_c \dot{q}_f - H_r \alpha_o). \tag{34}$$

According to the definition of a smooth curve: when a curve with a continuously turning tangent, which means it has a continuous first derivative on an interval, this curve will be smooth on this interval. Therefore, as long as (34) is satisfied, the trajectory of the object will have a continuous first derivative on an interval, and this trajectory will be smooth.

Remark 3: The necessary condition for stable grasp planning, as asserted by Theorem 2, serves as a foundational prerequisite for the dynamic manipulation. Any grasp planning associated with the specific grasp matrix G_C, meeting the conditions (existence of a solution for Equation (31) and full rank of G_C), guarantees the smooth and continuous trajectory of the grasped object during the manipulation.

V. THE DYNAMIC MODELING OF THE DEXTEROUS ROBOTIC HAND SUBJECT TO THE CONTACT CONSTRAINTS

A. THE ANALYTICAL DYNAMIC MODEL OF THE DEXTEROUS ROBOTIC HAND

Considering the robotic hand and the target object as an unified system, the dynamic model of the system obtained by the approach to multi-body system modeling introduced in [32]. According to this hierarchical and decentralized approach, the robotic hand manipulation system should be partitioned into four subsystems, comprising three finger subsystems and one object subsystem (considered as four "unconstrained" subsystems). Then, build the dynamic model of those "unconstrained" subsystems and formulate the constrained forces due to the contact constraints by the extended Udwadia-Kalaba equation.

Combining three finger subsystems and one object subsystem together yields

$$M(q, t)\ddot{q} = B\tau_f(t) + F(q, \dot{q}, t), \tag{35}$$

where M=blkdiag$[M_{f1}, M_{f2}, M_{f3}, M_o]$ ($M_{fi}(q_{fi}, t) \in R^{6\times6}$ and $M_o \in R^{12\times12}$ are the singular inertial matrix of the the ith finger subsystem and the object subsystem, respectively), $B = [I_{18\times18}; 0_{12\times18}]$, $\tau_f = [\tau_{f1}^T, \tau_{f2}^T, \tau_{f3}^T]^T$ ($\tau_{fi} = [\tau_{i1}, \tau_{i2}, \tau_{i3}, \tau_{i4}, 0, 0]^T$ is the control torques applied by the joint motors), $\ddot{q} = [\ddot{q}_{f1}^T, \ddot{q}_{f2}^T, \ddot{q}_{f3}^T, \ddot{q}_o^T]^T$ ($q_o = [x_o, y_o, z_o, \phi_o, \theta_o, \psi_o, \alpha_{o1}, \alpha_{o2}, \alpha_{o3}]^T$ is the re-selected coordinate of the object), and $F = [F_{f1}^T, F_{f2}^T, F_{f3}^T, F_o^T]^T$ ($F_{fi}(q_{fi}, \dot{q}_{fi}, t) \in R^6$ and $F_o \in R^{12}$ contain the centrifugal/Coriolis force and the gravity force of the four subsystems).

The second form of the pure rolling contact constraints (23) between the ith fingertip and the object can be expressed as follows:

$$A_{fi}\ddot{q}_{fi} + A_{oi}\ddot{q}_{oi} = -\dot{A}_{fi}\dot{q}_{fi} + \dot{A}_{oi}\dot{q}_{oi} =: b_{fi}. \tag{36}$$

Hence, the pure rolling contact constraints that the dexterous robotic hand manipulation system subject can be presented as

$$A_k \ddot{q} = b_k, \tag{37}$$

where $A_k = \begin{bmatrix} A_{f1} & \cdots & 0_{9\times6} & A_{ob1} \\ \vdots & A_{f2} & \vdots & A_{ob2} \\ 0_{9\times6} & \cdots & A_{f3} & A_{ob3} \end{bmatrix}$ and $b_k = \begin{bmatrix} b_{f1} \\ b_{f2} \\ b_{f3} \end{bmatrix}$. Here, $A_{ob1} = \begin{bmatrix} D_{o1} & 0_{3\times2} & 0_{3\times4} \\ 0_{3\times6} & -R_o(\partial^o C_{o1}/\partial\alpha_{o1}) & 0_{3\times4} \\ E_{o1} & R_o(\partial^o e_{o1}/\partial\alpha_{o1}) & 0_{3\times4} \end{bmatrix}$,

$A_{ob2} = \begin{bmatrix} D_{o2} & 0_{3\times2} & 0_{3\times2} & 0_{3\times2} \\ 0_{3\times6} & 0_{3\times2} & -R_o(\partial^o C_{o2}/\partial\alpha_{o2}) & 0_{3\times2} \\ E_{o2} & 0_{3\times2} & R_o(\partial^o e_{o2}/\partial\alpha_{o2}) & 0_{3\times2} \end{bmatrix}$, and $A_{ob3} = \begin{bmatrix} D_{o3} & 0_{3\times4} & 0_{3\times2} \\ 0_{3\times6} & 0_{3\times4} & -R_o(\partial^o C_{o3}/\partial\alpha_{o3}) \\ E_{o3} & 0_{3\times4} & R_o(\partial^o e_{o3}/\partial\alpha_{o3}) \end{bmatrix}$.

Since the inertia matrix M of the system is singular, suppose the Assumptions 1-2 are satisfied, the dynamic model of the robotic hand manipulation system under pure rolling contact constraints can be established by Theorem 1 as

$$\ddot{q} = \begin{bmatrix} (I - A_k^+ A_k)M \\ A_k \end{bmatrix} \begin{bmatrix} (I - A_k^+ A_k)(F + B\tau_f) \\ b_k \end{bmatrix}$$
$$=: \hat{M} \begin{bmatrix} (I - A_k^+ A_k)(F + B\tau_f) \\ b_k \end{bmatrix}. \tag{38}$$

According to lemma 2, $\hat{M}^+$ can be rewritten as

$$\hat{M}^+ = [M(I - A_k^+ A_k)M + A_k^T A_k]^{-1} \begin{bmatrix} (I - A_k^+ A_k)M \\ A_k \end{bmatrix}^T. \tag{39}$$

Substituting (39) in (38), the constrained force of the dexterous robotic hand manipulation system yields

$$F^c(q, \dot{q}, t) = M[M(I - A_k^+ A_k)M + A_k^T A_k]^{-1}$$
$$[M(I - A_k^+ A_k)(F + B\tau_f) + A_k^T b_k]$$
$$- (F + B\tau_f). \tag{40}$$

This constraint forces introduced in (40) is the pure rolling contact forces in the joint space, which is used to control the target object in the work space. To enhance the dynamic performance of the dexterous robotic hand manipulation system, it is essential to express the constrained forces, as stated in (40), within the workspace.

B. THE FINGERTIP CONTACT FORCES MODEL OF THE DEXTEROUS ROBOTIC HAND IN THE WORK SPACE

To determine the contact forces at the fingertip within the workspace, the dynamic model of the robotic hand manipulation system should be transformed into the work space at first. Set the position vector of the contact point C_i is $[x_{fci}, y_{fci}, z_{fci}]^T$ and reselect a set of independent coordinates $q_{xi} = [x_{fci}, y_{fci}, z_{fci}, \lambda_{1ci}, \lambda_{2ci}, \lambda_{3ci}]^T$ as the coordinates of the ith finger subsystem. Here, $\lambda_{1ci}, \lambda_{2ci}$, and λ_{3ci} are the

function of q_{fi}. Then, the relationship between q_{fi} and q_{xi} can be expressed as

$$\dot{q}_{xi} = \begin{bmatrix} \partial x_{f_{ci}}/\partial q_{fi} \\ \partial y_{f_{ci}}/\partial q_{fi} \\ \partial z_{f_{ci}}/\partial q_{fi} \\ \partial \lambda_{1ci}/\partial q_{fi} \\ \partial \lambda_{2ci}/\partial q_{fi} \\ \partial \lambda_{3ci}/\partial q_{fi} \end{bmatrix} \dot{q}_{fi} + \begin{bmatrix} \partial x_{f_{ci}}/\partial t \\ \partial y_{f_{ci}}/\partial t \\ \partial z_{f_{ci}}/\partial t \\ \partial \lambda_{1ci}/\partial t \\ \partial \lambda_{2ci}/\partial t \\ \partial \lambda_{3ci}/\partial t \end{bmatrix}$$

$$=: T_i(q_{fi}, t)\dot{q}_{fi} + k_i(q_{fi}, t), \quad (41)$$

where $T_i \in R^{6 \times 6}$ and $k_i \in R^6$.

Assumption 5: For any $(q_{fi}, t) \in R^6 \times R$, $T_i^{-1}(q_{fi}, t)$(i=1,2,3) exists.

Remark 4: According to (18), the position vector of the contact point C_i can be calculated by $q_{fi1}, q_{fi2}, q_{fi3}, q_{fi4}$, and α_{fi}. Hence, if $\lambda_{1ci}, \lambda_{2ci}$, and λ_{3ci} selected from those variables mentioned above, q_{xi} will be a set of independent coordinates as $\lambda_{1ci}, \lambda_{2ci}$, and λ_{3ci} be the function of q_{fi}.

If the hand robot manipulation system subjects to Assumption 5, according to (41), $\dot{q}_{fi}$ can be presented as

$$\dot{q}_{fi} = T_i^{-1}(\dot{q}_{xi} - k_i). \quad (42)$$

According to the definition of the virtual displacement introduced in Reference [29], there will be

$$\delta q_{fi} = T_i^{-1}\delta q_{xi}, \quad (43)$$

where δq_{fi} and δq_{xi} are virtual displacements. Take the derivative of (42), $\ddot{q}_{xi}$ can be given by

$$\ddot{q}_{xi} = \dot{T}_i\dot{q}_{fi} + T_i\ddot{q}_{fi} + \dot{k}_i. \quad (44)$$

By (44), $\ddot{q}_{fi}$ can be formulated as

$$\ddot{q}_{fi} = T_i^{-1}\ddot{q}_{xi} - T_i^{-1}(\dot{T}_i\dot{q}_{fi} + \dot{k}_i), \quad (45)$$

The joint space dynamic model for the ith finger subsystem, employs Lagrange's formulation of d'Alembert's principle, which asserts that the cumulative virtual work performed by the constraint force equals zero. Hence, the Fundamental Equation of ith finger subsystem will take the form of

$$\delta q_{fi}^T \left(M_{fi}\ddot{q}_{fi} - F_{fi} - \tau_{fi}\right) = 0. \quad (46)$$

Substituting (42), (43), and (45) in (46) yields

$$\delta q_{xi}^T T_i^{-T} \left[M_{fi}T_i^{-1}(\ddot{q}_{xi} - \dot{T}_iT_i^{-1}(\dot{q}_{xi} - k_i) - \dot{k}_i) - F_{fi} - \tau_{fi} \right]$$
$$= 0. \quad (47)$$

Let $M_{xi} := T_i^{-T}M_{fi}T_i^{-1}$, $F_{xi} := T_i^{-T}M_{fi}T_i^{-1}[\dot{T}_iT_i^{-1}(\dot{q}_{xi} - k_i) + \dot{k}_i] + T_i^{-T}F_{fi}$ and $\tau_{xi} := T_i^{-T}\tau_{fi}$. According to (47), the dynamic model of the ith "unconstrained" finger subsystem can be rewritten as

$$M_{xi}\ddot{q}_{xi} = F_{xi} + \tau_{xi}. \quad (48)$$

The dynamic model of the "unconstrained" target object in the workspace is still to be $M_o\ddot{q}_o = F_o$. Then, the dynamic model of the "unconstrained" dexterous robotic hand manipulation system can be established as

$$M_x\ddot{q}_x = F_x + \tau_x, \quad (49)$$

where M_x=blkdiag$(M_{x1}, M_{x2}, M_{x3}, M_o)$, $\ddot{q}_x = [\ddot{q}_{x1}^T, \ddot{q}_{x2}^T, \ddot{q}_{x3}^T, \ddot{q}_o^T]^T$, $F_x = [F_{x1}^T, F_{x2}^T, F_{x3}^T, F_o^T]^T$ and $\tau_x = [\tau_{x1}^T, \tau_{x2}^T, \tau_{x3}^T, 0_{1 \times 12}]^T$.

Comparing (49) with the dynamic model (35) in the joint space, there will be

$$M = T^T M_x T, \quad (50)$$

where T:=blkdiag$(T_1, T_2, T_3, I_{12 \times 12}) \in R^{30 \times 30}$. Suppose the Assumption 5 is satisfied, T^{-1} will exist and there will be

$$F + B\tau_f = T^T F_x - T^T M_x \dot{T} T^{-1} (\dot{q}_x - k)$$
$$- T^T M_x \dot{k} + T^T \tau_x, \quad (51)$$

where $k := [k_1^T, k_2^T, k_3^T, 0_{1 \times 12}]^T$.

Set the pure rolling contact constraints between the ith finger and object in the work space can be rewritten as

$$A_{xi}\dot{q}_{xi} + A_{oi}\dot{q}_{oi} + c_{xi} = 0. \quad (52)$$

Taking the derivative of (52) yields

$$A_{xi}\ddot{q}_{xi} + A_{oi}\ddot{q}_{oi} = -\dot{A}_{xi}\dot{q}_{xi} - \dot{A}_{oi}\dot{q}_{oi} - \dot{c}_{xi} =: b_{xi}. \quad (53)$$

Plugging (42) and (44) into (53) will obtain

$$A_{xi}T_i\ddot{q}_{fi} + A_{oi}\ddot{q}_{oi} = b_{xi} - A_{xi}[\dot{T}_iT_i^{-1}(\dot{q}_{xi} - k_i) + \dot{k}_i]. \quad (54)$$

Compare (54) with the contact constraints (36), there will be $A_{fi} = A_{xi}T_i$ and $b_{fi} = b_{xi} - A_{xi}\left[\dot{T}_iT_i^{-1}(\dot{q}_{xi} - k_i) + \dot{k}_i\right]$. Hence, the contact constraints suffered by the dexterous robotic hand manipulation system in the work space can be given by

$$A_x\ddot{q}_x = b_x, \quad (55)$$

where $A_x = \begin{bmatrix} A_{x1} & \cdots & 0_{9 \times 6} & A_{ob1} \\ \vdots & A_{x2} & \vdots & A_{ob2} \\ 0_{9 \times 6} & \cdots & A_{x3} & A_{ob3} \end{bmatrix}$ and $b_x = [b_{x1}^T, b_{x2}^T, b_{x3}^T]^T$. Besides, A_k, b_k, A_x, and b_x will satisfied the follow relationships:

$$\begin{cases} A_k = A_x T, \\ b_k = b_x - A_x \dot{T} T^{-1} (\dot{q}_x - k) - A_x \dot{k}. \end{cases} \quad (56)$$

Suppose the dexterous robotic hand manipulation system subject to Assumptions 1-2 in the work space, according to Theorem 1, the acceleration coordinates $\ddot{q}_x$ of the system under pure rolling contact constraints (55) can be formulated as

$$\ddot{q}_x = \begin{bmatrix} (I - A_x^+A_x)M_x \\ A_x \end{bmatrix}^+ \begin{bmatrix} (I - A_x^+A_x)(F_x + \tau_x) \\ b_x \end{bmatrix}. \quad (57)$$

According to (57), the fingertip contact forces in the work space can be presented as

$$F_x^c = M_x \begin{bmatrix} (I - A_x^+A_x)M_x \\ A_x \end{bmatrix}^+ \begin{bmatrix} (I - A_x^+A_x)(F_x + \tau_x) \\ b_x \end{bmatrix}$$

$$- (F_x + \tau_x). \tag{58}$$

Assumption 6: For any $(q,t) \in R^{30} \times R$, $(TT^T - I)^{-1}$ exists.

Theorem 3: if the dexterous robotic hand manipulation system (49), which is under the contact constraints (55), is subject to Assumptions 1-2 and 5-6, the contact forces $F_x^c \in R^{30}$ in the work space can be computed based on the constrained forces $F^c \in R^{30}$ in the joint space as

$$F_x^c = (TT^T - I)^{-1}(I + \tilde{P})(TT^T - I)T^{-T}F^c, \tag{59}$$

where $\tilde{P} := (TT^T - I)M_x[M_x(I - A_x^+ A_x)M_x + A_x^T A_x]^{-1} M_x(I - A_x^+ A_x)$.

Proof of Theorem 3: When the Assumption 1 is satisfied, the constrained forces F^c of the hand robot manipulation system can be deduced as (40) by lemma 2. Besides, if $\hat{M}$ has full column rank, $\begin{bmatrix} M \\ A_k \end{bmatrix}$ will also be full column matrix according to lemma 1. Under Assumption 5, there will be $A_x = A_k T^{-1}$ and $M_x = T^{-T}MT^{-1}$ based on (56). Then, $\begin{bmatrix} M_x \\ A_x \end{bmatrix}$ can be rewritten as

$$\begin{bmatrix} M_x \\ A_x \end{bmatrix} = \begin{bmatrix} T^{-T}MT^{-1} \\ A_k T^{-1} \end{bmatrix} = \begin{bmatrix} T^{-T} \\ & I_{9 \times 9} \end{bmatrix} \begin{bmatrix} M \\ A_k \end{bmatrix} T^{-1}. \tag{60}$$

If $\begin{bmatrix} M \\ A_k \end{bmatrix}$ is column non-singular, $\begin{bmatrix} M_x \\ A_x \end{bmatrix}$ will have full column rank. Therefore, $\begin{bmatrix} (I - A_x^+ A_x)M_x \\ A_x \end{bmatrix}$ will be a full column matrix according to lemma 1. Using lemma 2, (58) can be simplified as

$$F_x^c = M_x[M_x(I - A_x^+ A_x)M_x + A_x^T A_x]^{-1} \\ [M_x (I - A_x^+ A_x)(F_x + \tau_x) + A_x^T b_x] - (F_x + \tau_x). \tag{61}$$

Plugging (50), (51), and (56) into (40) yields

$$F^c = T^T M_x[M_x T(I - (A_x T)^+ A_x T)T^T M_x + A_x^T A_x]^{-1} \\ [M_x T(I - (A_x T)^+ A_x T)T^T(F_x + \tau_x) + A_x^T b_x] \\ - T^T (F_x + \tau_x). \tag{62}$$

Using lemma 3, $(A_x T)^+$ in (62) can be rewritten as

$$(A_x T)^+ = T^+ \left(A_x^+ A_x TT^+ \right)^+ A_x^+. \tag{63}$$

Since T^{-1} exists according to Assumption 5, there will be $T^+ = T^{-1}$ and (63) can be simplified based on lemma 4 as

$$(A_x T)^+ = T^{-1} A_x^+. \tag{64}$$

Substitute (64) in (61), the constrained forces F^c can be calculated as

$$F^c = T^T M_x \left[M_x(I - A_x^+ A_x)TT^T M_x + A_x^T A_x \right]^{-1} \\ \left[M_x(I - A_x^+ A_x)TT^T (F_x + \tau_x) + A_x^T b_x \right] \\ - T^T (F_x + \tau_x). \tag{65}$$

In order to simplify (65), $[M_x(I - A_x^+ A_x)TT^T M_x + A_x^T A_x]^{-1}$ should be dealt first. It can be rewritten as

$$\left[M_x(I - A_x^+ A_x)TT^T M_x + A_x^T A_x \right]^{-1} \\ = \left[M_x(I - A_x^+ A_x)(TT^T - I)M_x \\ + M_x(I - A_x^+ A_x)M_x + A_x^T A_x \right]^{-1}. \tag{66}$$

Let $\tilde{D} = M_x \left(I - A_x^+ A_x \right) M_x + A_x^T A_x$ and $\tilde{D}^{-1}$ exists, $\tilde{U} = M_x(I - A_x^+ A_x)$, $\tilde{O} = (TT^T - I)$, and $\tilde{V} = M_x$. If the system subjects to Assumption 6, $\tilde{O}^{-1}$ will exist. Using lemma 5, the right part of (66) can be conducted as

$$\left[M_x(I - A_x^+ A_x)(TT^T - I)M_x + M_x(I - A_x^+ A_x)M_x + A_x^T A_x \right]^{-1} \\ = \left[M_x(I - A_x^+ A_x)M_x + A_x^T A_x \right]^{-1} - \\ \left[M_x(I - A_x^+ A_x)M_x + A_x^T A_x \right]^{-1} M_x(I - A_x^+ A_x) \times \\ \left[I + (TT^T - I)M_x[M_x(I - A_x^+ A_x)M_x + A_x^T A_x]^{-1} M_x(I - A_x^+ A_x) \right]^{-1} \\ (TT^T - I)M_x \left[M_x(I - A_x^+ A_x)M_x + A_x^T A_x \right]^{-1}. \tag{67}$$

According to (13), $\left[I + (TT^T - I)M_x[M_x(I - A_x^+ A_x)M_x + A_x^T A_x]^{-1}M_x(I - A_x^+ A_x) \right]^{-1}$ exists, which means $(I + \tilde{P})^{-1}$ exists. Substitute (67) in (65) and use lemma 6 to get

$$F^c = T^T F_x^c - T^T(TT^T - I)^{-1}\tilde{P}(I + \tilde{P})^{-1}(TT^T - I)F_x^c \\ = T^T(TT^T - I)^{-1} \left[I - \tilde{P}(I + \tilde{P})^{-1} \right] (TT^T - I)F_x^c \\ = T^T(TT^T - I)^{-1}(I + \tilde{P})^{-1}(TT^T - I)F_x^c. \tag{68}$$

Since T^{-1}, $(TT^T - I)^{-1}$, and $(I + \tilde{P})^{-1}$ exist, $\left[T^T(TT^T - I)^{-1}(I + \tilde{P})^{-1}(TT^T - I) \right]^{-1}$ will exist. Hence, the contact forces in the work space can be presented as $F_x^c = (TT^T - I)^{-1}(I + \tilde{P})(TT^T - I)T^{-T}F^c$.

Remark 5: Theorem 3 introduces the relationship between the pure rolling contact forces F_x^c in the work space and the constrained forces F^c in the joint space. According to (59), it can be seen that the fingertips contact forces F_x^c are only dependent on the generalized variables q and $\dot{q}$. Compared with traditional manipulation control methods that measure the contact forces by the force sensors, Theorem 3 provides a new approach for the dexterous robotic hand manipulation system to formulate the fingertip contact forces, which offers the potential to develop dynamic manipulation control system without the necessity of using force information.

VI. THE DYNAMIC MANIPULATION CONTROL DESIGN OF THE DEXTEROUS ROBOTIC HAND

To manipulate the target object tracking the desired trajectory, the dynamic control designed based on the contact forces needs to provide the appropriate finger joint driving torques. Before the control design, the dynamics modeling (38) of the

dexterous robotic hand manipulation system using lemma 2 can be decoupled as

$$\ddot{q} = \left[M(I - A_k^+ A_k)M + A_k^T A_k\right]^{-1}\left[M(I - A_k^+ A_k)F + A_k^T b_k\right] +$$
$$\left[M(I - A_k^+ A_k)M + A_k^T A_k\right]^{-1}M(I - A_k^+ A_k)B\tau_f. \quad (69)$$

A. CONTROL DESIGN FOR DYNAMIC MANIPULATION

Suppose the desired trajectory of the object to be $q_o^d = [x_o^d, y_o^d, z_o^d] \in R^3$, the desired velocity and acceleration to be $\dot{q}_o^d$ and $\ddot{q}_o^d$. Then, the error between the actual position of the object and the desired trajectory q_o^d can be presented as

$$e(q_o, \dot{q}_o, t) = q_o - q_o^d. \quad (70)$$

To track the desired trajectory with the intended velocity, the servo constraints can be formulated as

$$\dot{e}(q_o, \dot{q}_o, t) + Ke(q_o, t) = 0, \quad (71)$$

where the constant matrix $K = \text{diag}[k_i]_{3\times3}$, $k_i > 0$, $k_i = \lambda_{\min}(K) (i = 1, \cdots, 3)$. Here, $\lambda_{\min}(\cdot)$ stands for the minimum eigenvalue of the designated matrix.

Differentiating the servo constraints (71) with respect to t yields

$$\ddot{e}(q_o, \dot{q}_o, t) + K\dot{e}(q_o, \dot{q}_o, t) = 0. \quad (72)$$

Equation (72) can be represented in the form of matrix as

$$A_s\ddot{q} = b_s(q, \dot{q}, t), \quad (73)$$

where $A_s = [0_{3\times18}, I_{3\times3}, 0_{3\times9}]$ and $b_s = \ddot{q}_o^d - K(\dot{q}_o - \dot{q}_o^d)$.

Assumption 7: Equation (73) is consistent: for any $A_s(q, t)$ and $b_s(q, \dot{q}, t)$, there exists at least one solution $\ddot{q}$ to (73).

Remark 6: According to Assumption 7, there will be $A_s A_s^+ b_s = b_s$.

According to the dynamic model of the dexterous robotic hand manipulation system (69) and the servo constraints (73), there can be

$$A_s\Phi\tau_f = \bar{b}, \quad (74)$$

where $\Phi = [M(I - A_k^+ A_k)M + A_k^T A_k]^{-1}M(I - A_k^+ A_k)B$ and $\bar{b} = b_s - A_s[M(I - A_k^+ A_k)M + A_k^T A_k]^{-1}[M(I - A_k^+ A_k)F + A_k^T b_k]$. Equation (74) can be consider as a constraint for the control torques τ_f.

Assumption 8: Equation (74) is consistent: for any $A_s(q, t)$, $\Phi(q, t)$ and $\bar{b}(q, \dot{q}, t)$, there exists at least one solution τ_f to (74).

Remark 7: According to Assumption 8, there will be $A_s\Phi(A_s\Phi)^+\bar{b} = \bar{b}$.

Theorem 4: Subject to Assumptions 7-8, the dynamic model of the mechanical system (69) is servo constraints controllable for the constraints (73) if and only if

$$Rank[A_s(q, t)\Phi(q, \dot{q}, t)] \geq 1, \quad (75)$$

for any $(q, \dot{q}, t) \in R^{30} \times R^{30} \times R$. Furthermore, for all $(q, \dot{q}, t) \in R^{30} \times R^{30} \times R$, the constraint-following control τ_f can be presented as

$$\tau_f = (A_s\Phi)^+\bar{b} + \left[I - (A_s\Phi)^+ A_s\Phi\right]S, \quad (76)$$

where $S \in R^{30}$ is an arbitrary vector.

Proof of Theorem 4: (Sufficiency) Suppose $\text{Rank}[A_s(q, t)\Phi(q, \dot{q}, t)] \geq 1$, which means $[A_s(q, t)\Phi(q, \dot{q}, t)]^+$ exists according to [29] and the control (76) is meaningful. Using the constraint-following control τ_f in system (69) and multiplying both sides of (69) by A_s result in

$$A_s\ddot{q} = A_s\left[M(I - A_k^+ A_k)M + A_k^T A_k\right]^{-1}$$
$$\left[M(I - A_k^+ A_k)F + A_k^T b_k\right] + A_s\Phi\tau_f$$
$$= b_s - \bar{b} + A_s\Phi\left[(A_s\Phi)^+\bar{b} + [I - (A_s\Phi)^+ A_s\Phi]S\right]$$
$$= b_s \underbrace{-\bar{b} + A_s\Phi(A_s\Phi)^+\bar{b}}_{=0} + \underbrace{[A_s\Phi - A_s\Phi(A_s\Phi)^+ A_s\Phi]}_{=0}S$$
$$= b_s. \quad (77)$$

(Necessity) Suppose that $\text{Rank}[A_s(q, t)\Phi(q, \dot{q}, t)] = 0$ for some $(q, \dot{q}, t)$, which means $A_s(q, t)\Phi(q, \dot{q}, t) = 0$ for some $(q, \dot{q}, t)$. Pre-multiplying both sides of (69) by A_s, since $A_s\Phi = 0$ for some $(q, \dot{q}, t)$, there will be

$$A_s\ddot{q} = A_s\left[M(I - A_k^+ A_k)M + A_k^T A_k\right]^{-1}$$
$$\left[M(I - A_k^+ A_k)F + A_k^T b_k\right]$$
$$= b_s - \bar{b}. \quad (78)$$

It can be seen that (78) is not equal to the servo constraints (73). Hence, $\text{Rank}[A_s(q, t)\Phi(q, \dot{q}, t)] \geq 1$ should be satisfied for all $(q, \dot{q}, t) \in R^{30} \times R^{30} \times R$.

Remark 8: The dexterous robotic hand manipulation system is considered a typical under-drive system because it has fewer finger joint driving torques than the number of coordinates chosen to describe its motion. Based on the constraint-following control method, paper [33] introduced a control designing method for such an under-drive system with a non-singular inertia matrix. However, the inertia matrix M of the dexterous robotic hand manipulation system under pure rolling contact constraints is singular, which means the inverse of M cannot be solved. Compared with the controller proposed in paper [33], the constraint-following control (76) introduced in Theorem 2 can accomplish the manipulation tasks even when the inertia matrix of the system does not have a full rank.

Assumption 9: For a given constant matrix $P \in R^{3\times3}$, $P > 0$, there exists a constant $\lambda > 0$ such that

$$\lambda_{\min}(PA_s(q, t)\Phi(q, \dot{q}, t)(A_s(q, t)\Phi(q, \dot{q}, t))^T P^T) \geq \lambda. \quad (79)$$

Remark 9: According to Assumption 9, the minimum eigenvalue of the matrix $(PA_s(q, t)\Phi(q, \dot{q}, t)(A_s(q, t)\Phi(q, \dot{q}, t))^T P^T)$ needs to be large than 0, which implies that the matrix $(PA_s(q, t)\Phi(q, \dot{q}, t)(A_s(q, t)\Phi(q, \dot{q}, t))^T P^T)$ will be symmetrically positively definite for any $(q, \dot{q}, t) \in R^{30} \times R^{30} \times R$.

Set the servo constraints error of the dexterous robotic hand manipulation system as $\nu(t) := \dot{e}(q_o, \dot{q}_o, t) + Ke(q_o, t)$. Based on the Theorem 2, the dynamics manipulation control of the system which is suffered by the pure rolling contact

constraints is proposed as

$$\tau_f(t) = p_1(q, \dot{q}, t) + p_2(q, \dot{q}, t), \quad (80)$$

with

$$p_1(q, \dot{q}, t) = [A_s(q, t)\Phi(q, \dot{q}, t)]^+ \bar{b}(q, \dot{q}, t), \quad (81)$$

$$p_2(q, \dot{q}, t) = -\gamma [A_s(q, t)\Phi(q, \dot{q}, t)]^T P^T v(t), \quad (82)$$

where the constant $\gamma > 0$.

B. STABILITY ANALYSIS OF DESIGNED CONTROL STRATEGY

Choose the Lyapunov function as

$$V(v) = v^T P v, \quad (83)$$

where the constant matrix $P > 0$. Then, there will be $V \geq ||v||^2$.

Since $V(0, t) = 0$ and $V(v, t) > 0$ when $v \neq 0$, the function V in (83) is said to be decrescent.

Taking the derivative of (83) yields

$$\dot{V} = 2v^T P\dot{v} = 2v^T P(A_s\ddot{q} - b_s). \quad (84)$$

With the proposed control design (80), $(A_s\ddot{q} - b_s)$ in (84) can rewritten according to Assumption 8 as

$$A_s\ddot{q} - b_s$$
$$= \underbrace{A_s\Phi(A_s\Phi)^+\bar{b} - \bar{b}}_{=0} - \gamma A_s\Phi(A_s\Phi)^T P^T v$$
$$= -\gamma A_s\Phi(A_s\Phi)^T P^T v. \quad (85)$$

Substitute (85) in (76) to get

$$\dot{V} = -2\gamma v^T P A_s\Phi(A_s\Phi)^T P^T v. \quad (86)$$

According to Assumption 9, (86) can be rewritten as

$$\dot{V} \leq -2\gamma\lambda v^T v = -2\gamma\lambda||v||^2. \quad (87)$$

Since $\gamma > 0$, $\lambda > 0$, $\dot{V}(v, t) = 0$ only when $v = 0$, and $\dot{V}(v, t) < 0$ with $\forall v \neq 0$, the constraint-following error $v(t)$ is uniformly stable.

Suppose there exists a constant $\delta > 0$ for $||v(t_1) - v(t_2)|| < \delta$, the following equation based on (87) will be satisfied:

$$\dot{V}_1 - \dot{V}_2 \leq 2\gamma\lambda(||v(t_2)||^2 - v(t_1)||^2)$$
$$= 2\gamma\lambda(||v(t_2) - v(t_1)|| ||v(t_2) + v(t_1)||)$$
$$< 2\gamma\lambda\delta||v(t_2) + v(t_1)||. \quad (88)$$

According to the definition of uniformly stable: $||v(t)|| < \hat{k}$ for any $t > t_0$, (88) can be rewritten as

$$\dot{V}_1 - \dot{V}_2 < 2\gamma\lambda\delta||v(t_2) + v(t_1)|| < 4\gamma\lambda\delta\hat{k}. \quad (89)$$

Hence, the function $\dot{V}(v, t)$ will be uniformly continuous at time t. Besides, since $V(v, t) \geq 0$ is lower unbounded and $\dot{V}(v, t) \leq 0$ is negative semi-definite, there will be $\dot{V}(v, t) = -2\gamma\lambda||v||^2 \rightarrow 0$ as $t \rightarrow \infty$ according to the Lyapunov-Like lemma discussed in [34], which means $lim_{t\rightarrow\infty} v(t) = 0$.

TABLE 1. The Properties of the dexterous robotic hand manipulation system.

Symbol	Means	Data	Unit
m_1	the proximal phalanx's mass	0.06	kg
m_2	the middle phalanx's mass	0.033	kg
m_3	the distal phalanx's mass	0.018	kg
m_o	the target object's mass	0.053	kg
r_1	the fingertip's radius	10	mm
r_2	the target object's radius	30	mm
l	the phalanx's length	40	mm
g	gravitational acceleration	9800	mm/s^2

TABLE 2. The simulation parameters of the dexterous robotic hand manipulation system.

Symbol	Data	Unit
q_{f1}	[-1.513689; 1.439038; 0.346388; -2.039030; 0.066831; 1.792217]	rad
q_{f2}	[2.5408120; 1.621548; -0.158905; -1.695082; -0.0347450; 1.705898]	rad
q_{f3}	[0.601601; 1.919066; -0.806517; -1.204788; 0.082720; 1.647304]	rad
q_o	[1.632884; 4.672300; 69.422381; -0.041982; 1.535519; -0.032036; -0.020233; 1.645094; 1.034046; -1.659032; -1.018308; -1.618006]	mm or rad
$\dot{q}_{f1}$	[0.089534; -1.089919; 2.439512; -1.386070; 0.052346; 0.059651]	rad/s
$\dot{q}_{f2}$	[-0.226253; -0.567053; 0.950041; -0.908325; -0.185272; 0.368132]	rad/s
$\dot{q}_{f3}$	[0.106493; 0.247942; -0.737890; 0.691595; 0.017312; 0.104417]	rad/s
$\dot{q}_o$	[4.082141; 10.429187; -0.777873; -0.043177; -0.011827; 0.019302; -0.016664; 0.020479; -0.071678; -0.229078; 0.017312; 0.104417]	mm/s or rad/s

Remark 10: Consider the dexterous robotic hand manipulation system (69), which is under pure rolling contact constraints, subjects to Assumptions 7-9. Under the constraint-following control (80), the following performance of the target object trajectory tracking error $v(t) = \dot{e}(q_o, \dot{q}_o, t) + Ke(q_o, t)$ is guaranteed: (t_0 is the initial time)

(1) Uniformly stability: for any $\hat{k} > 0$ ($\hat{k}$ is a constant) and $||v(t_0)|| < \hat{k}$, there will be $||v(t)|| < \hat{k}$ as $t > t_0$.

(2) Converge to zero: for any $t > t_0$, $lim_{t\rightarrow\infty} v(t) = 0$.

The design dynamic control (80) of the dexterous robotic hand manipulation system includes two portions: The feed-forward portion (81), which is formulated by the contact forces model, and the feedback portion (82) that can eliminate the initial constraint-following error. With the introduced control method, the robotic hand can achieve precise tracking of the target object's trajectory without relying on the feedback information from force sensors for contact force.

The architecture of dynamic modeling and control strategy for the hand-object manipulation system is presented in Appendix B.

VII. SIMULATION AND DISCUSSION
A. SIMULATION SETUP

To verify the dynamic modeling and control design of the dexterous robotic hand, the three-fingered dexterous robotic hand manipulating a target, depicted in Fig. 1, is simulated
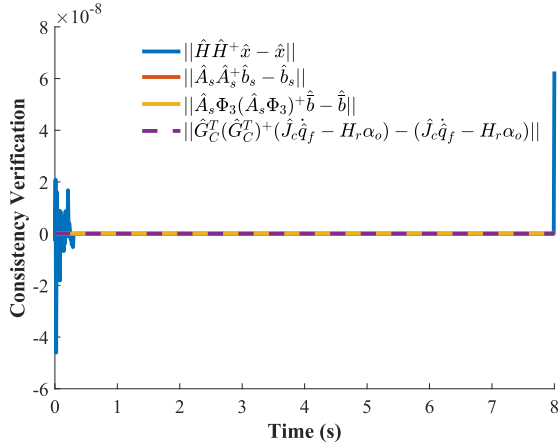
FIGURE 4. The consistency verification.

FIGURE 5. The rank of those matrixs.

FIGURE 6. The minimum eigenvalue of the matrix $(P\bar{B}(q,t)\bar{B}^T(q,t)P^T)$.

FIGURE 7. The trajectory of the object.

in MATLAB. The dynamics model and the controller are numerically solved by the ordinary differential equation solver ode45 which is a general Runge-Kutta method solver.

The robotic hand comprises three identical fingers which physical properties are listed in Table 2. Additionally, Table 3 illustrates the initial conditions of the three fingers and the target in the simulation. Set the desired trajectory as $q_o^d = [2, 6, 40\sqrt{3}]^T$ and the control parameters as $\gamma = 10$ and K=diag(8,8,8).

Moreover, a comparative experiment is conducted by the control strategy introduced in [35], in which a task-oriented manipulation control is designed as

$$\tau_f^t = L_{k1}[A_s(q,t)\Phi(q,\dot{q},t)]^T[k_2 e(q_o,\dot{q}_o,t) + \dot{e}(q_o,\dot{q}_o,t)]$$

$$+ L_c[A_s(q,t)\Phi(q,\dot{q},t)]^T[x_o^d, y_o^d, z_o^d]^T. \quad (90)$$

Here, $L_{k1} = -20$, $k_2 = 15$, and $L_c = 2$ are control parameters.

B. RESULTS AND DISCUSSION
The simulation results of the dexterous robotic hand manipulation system are demonstrated in Fig. 4-Fig. 23. Furthermore, simulation results Fig. 4-Fig. 6 are intended to verify the assumptions proposed during early stage the dynamic modeling and control design (section VI-VII). Fig. 7 and Fig. 8 represent the manipulation control performance of the proposed control strategy (80) and state feedback control strategy (90).

With Assumptions 2-3 and 7-8, equations (5), (31), (73), and (74) must remain consistent to ensure the existence of solutions. This implies $\hat{M}\hat{M}^+\xi = \xi$ where $\xi := \begin{bmatrix} (I - A_k^+ A_k)(F + B\tau_f) \\ b_k \end{bmatrix}$, $G_C^T(G_C^T)^+(J_c\dot{q}_f - H_r\alpha_o) = (J_c\dot{q}_f - H_r\alpha_o)$, $A_s A_s^+ b_s = b_s$, and $A_s\Phi(A_s\Phi)^+\bar{b} = \bar{b}$.

According to Fig. 4, it is evident that the orders of magnitude for $||\hat{M}\hat{M}^+\xi - \xi||$, $||G_C^T(G_C^T)^+(J_c\dot{q}_f - H_r\alpha_o) - (J_c\dot{q}_f - H_r\alpha_o)||$, $||A_s A_s^+ b_s - b_s||$, and $||A_s\Phi(A_s\Phi)^+\bar{b} - \bar{b}||$ are at 10^{-8} during the simulation time interval, indicating the fulfillment of Assumptions 2-3 and 7-8.
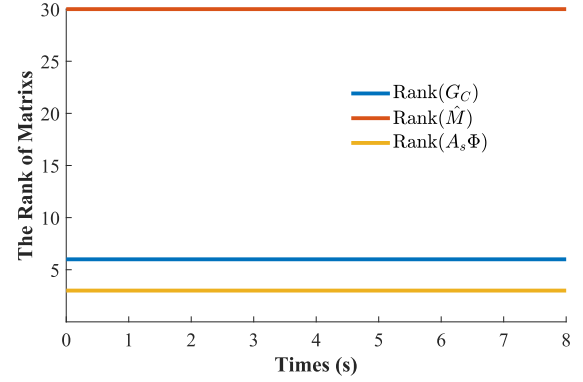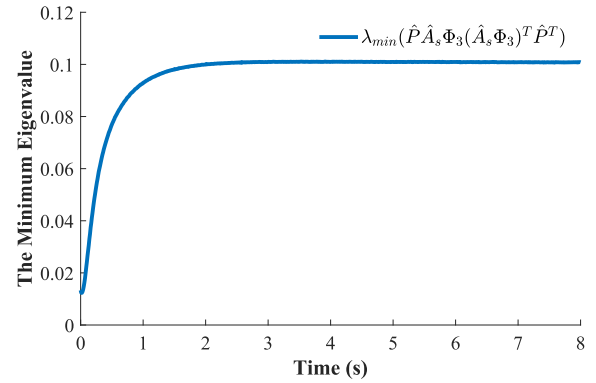
Fig. 5 demonstrates that the matrix $\hat{M}$ has a rank of 30, confirming the Assumption 1. Additionally, as outlined in Theorem 4, the matrix $A_s\Phi$ should have a rank greater than 1, which is also confirmed in Fig. 5 during the simulation interval. Furthermore, the matrix G_c achieves a rank of 6, satisfying the Assumption 4. According to Theorem 2, the proposed grasp planning method ensures a trajectory for the target object that remains smooth and continuous.

Fig. 6 indicates that the minimum eigenvalue of the matrix $(PA_s\Phi(A_s\Phi)^T P^T)$ remains greater than 0, which means the Assumption 9 is satisfied during the simulation period.
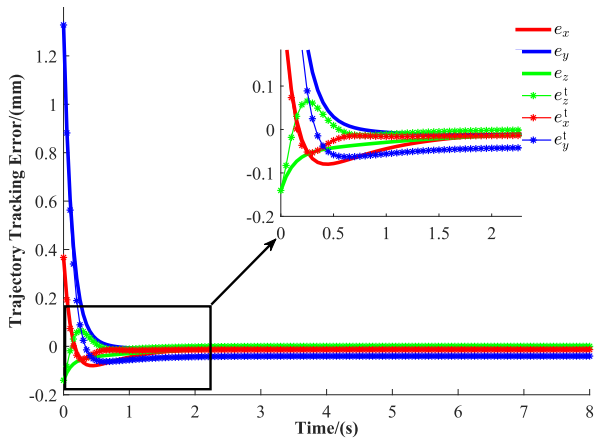
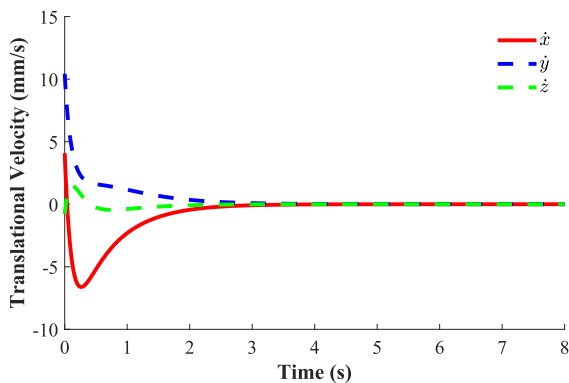**FIGURE 8.** The trajectory tracking error.
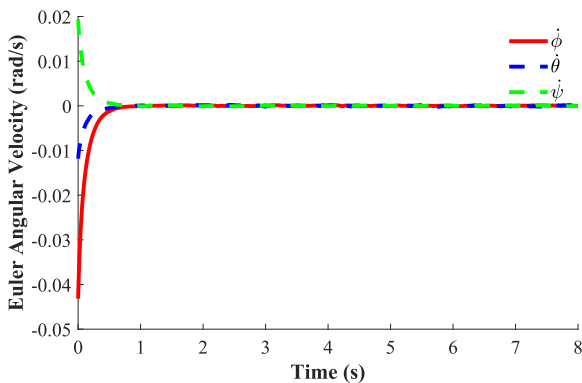

FIGURE 9. The translational velocity of the object.
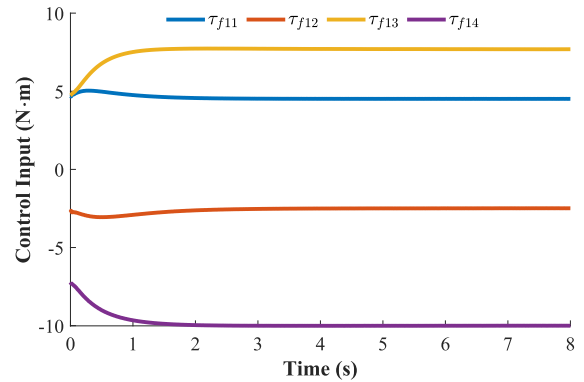

FIGURE 10. Euler angular velocity of the object.

FIGURE 11. The control input of finger 1.
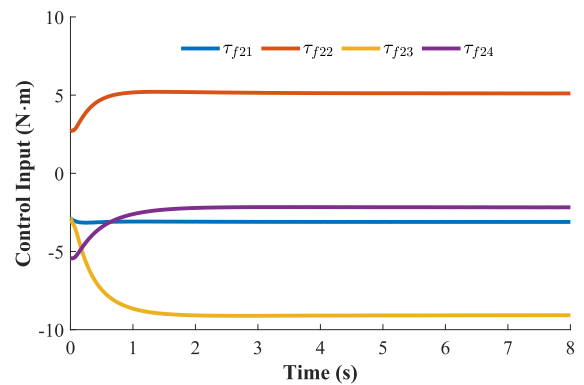
FIGURE 12. The control input of finger 2.
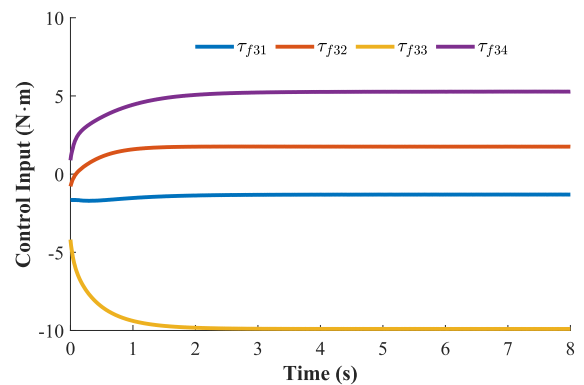
FIGURE 13. The control input of finger 3.

Hence, with the design control (80), the dexterous robotic hand manipulation system under pure rolling contact constraints is always subjects to those Assumptions that needed for the dynamics modeling and control design.

After verifying these assumptions, the manipulation performance of the control (80) and (90) is illustrated in Fig. 7 and Fig. 8. In Fig. 7, the trajectory of the target object under the proposed control strategy is represented by the blue line, while the trajectory under the task-oriented manipulation control strategy is depicted by the yellow line. The green point marks the initial position of the object's center of mass, and the red one marks its desired position. Let $e := [e_x, e_y, e_z]^T$ and $e^t := [e_x^t, e_y^t, e_z^t]^T$ represent the tracking errors under the proposed control strategy (80) and task-oriented manipulation control strategy (90). Fig. 8 illustrates the trajectory tracking error between the object's center of mass's current and intended positions. The tracking error e under the proposed control strategy (80) significantly diminishes, approaching zero after 2 seconds. In contrast, the tracking error e^t under the task-oriented manipulation control
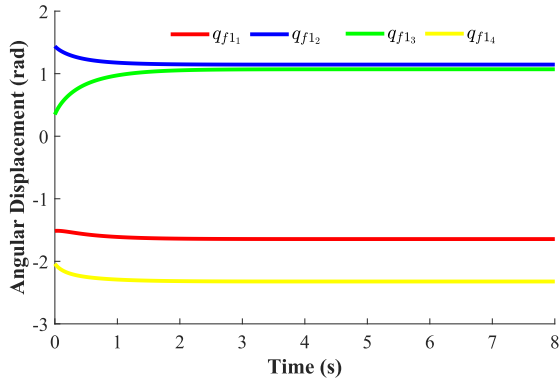
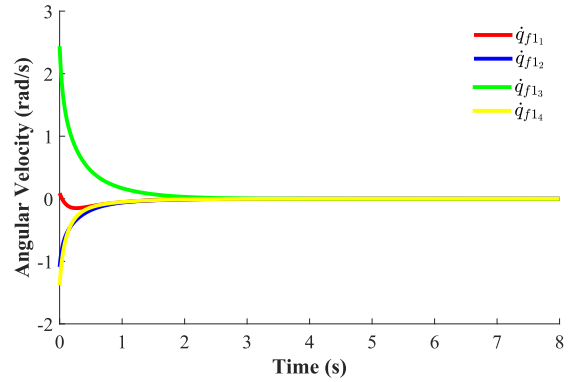**FIGURE 14.** The angular displacement of finger 1.

FIGURE 15. The angular displacement of finger 2.
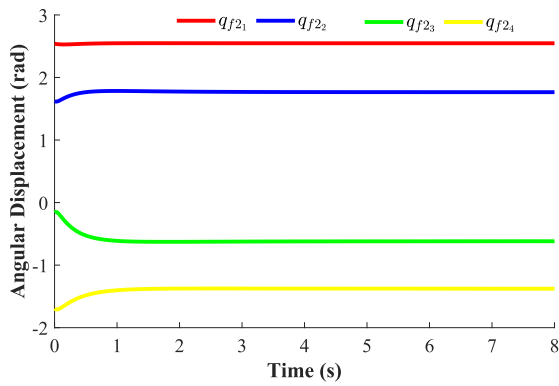

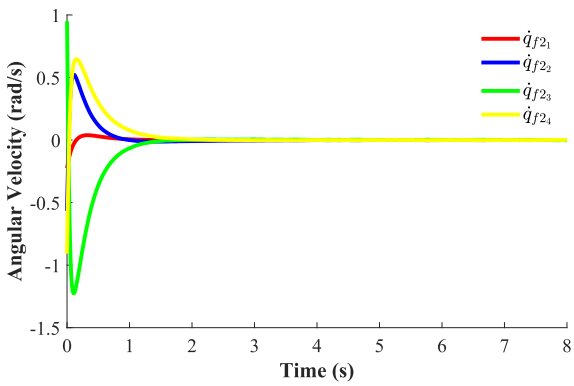**FIGURE 16.** The angular displacement of finger 3.

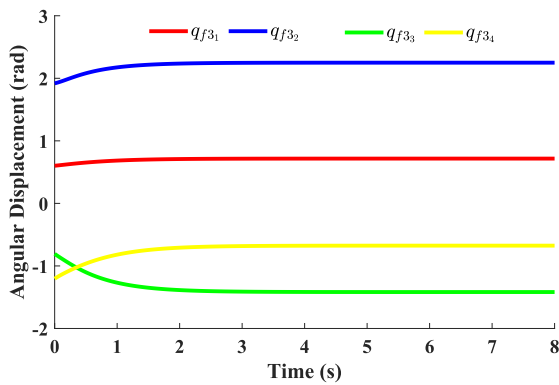**FIGURE 17.** The angular velocity of finger 1.

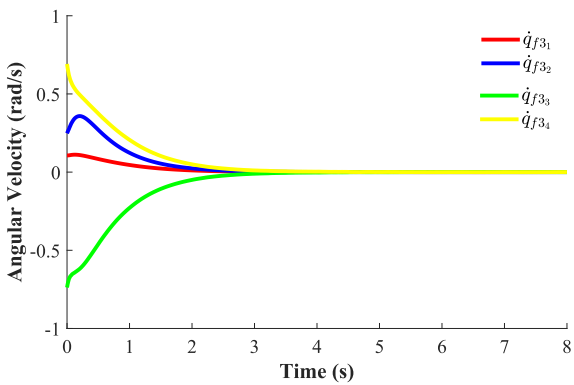**FIGURE 18.** The angular velocity of finger 2.

FIGURE 19. The angular velocity of finger 3.

strategy (90) exhibits a steady-state error of 0.04mm in the y-direction.

The manipulation task requires a high level of control precision, particularly in accurate positioning and handling. In this context, the proposed control strategy (80) stands out as the superior choice compared to the (90). Despite requiring a longer execution time, the extended duration facilitates refinement and precision correction, ensuring precise control throughout the manipulation task. While the task-oriented manipulation control strategy (90) achieves a relatively shorter completion time, the presence of a 0.04mm

steady-state error may limit its applicability, particularly in tasks where minimizing deviation is critical. Hence, for tasks requiring high precision, the proposed control strategy (80) demonstrates superior operational efficacy compared to (90).

The detailed simulation results under the proposed control strategy (80) are represented in Fig. 9-Fig. 23. The translational and angular velocity of the object displayed in Fig. 9 and Fig. 10. The control torques τ_{f1}, τ_{f2}, and τ_{f3} applied on the finger joints are shown in Fig. 11-Fig. 13, where $\tau_{fi} = [\tau_{fi1}, \tau_{fi2}, \tau_{fi3}, \tau_{fi4}]$(i=1,2,3). The torque applied to each finger is limited to a maximum of $8\ N \cdot m$, making it suitable
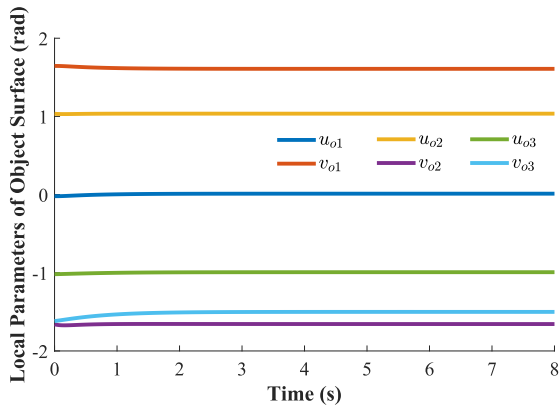
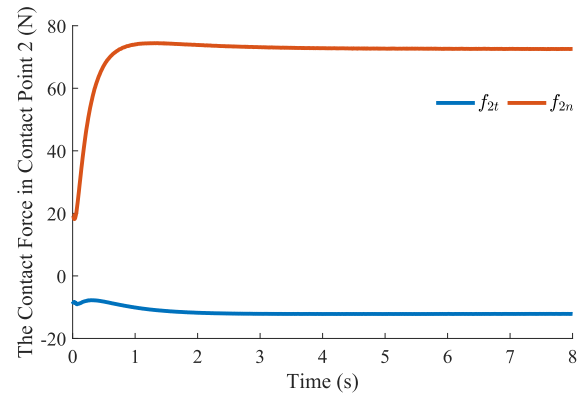**FIGURE 20.** The angular displacement of local parameters of the object surface.
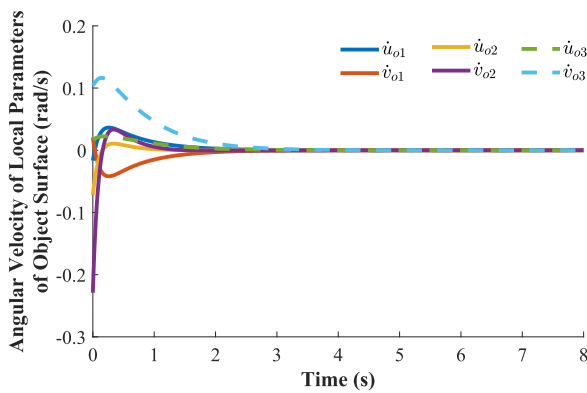

FIGURE 21. The angular velocity of local parameters of the object surface.

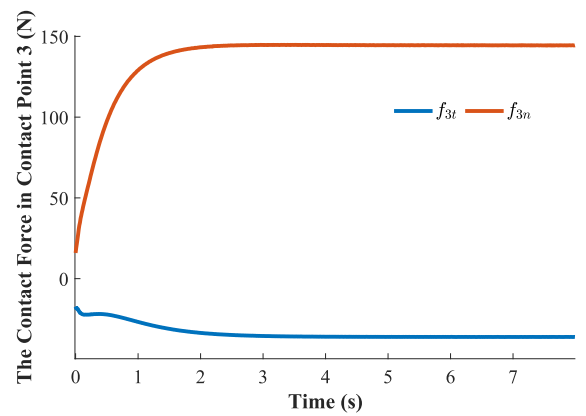**FIGURE 22.** The contact force in contact point 1.

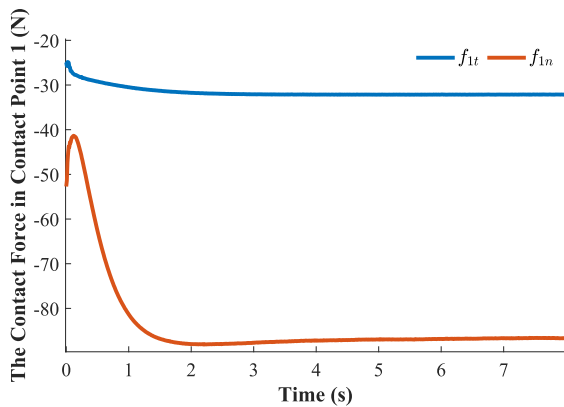**FIGURE 23.** The contact force in contact point 2.

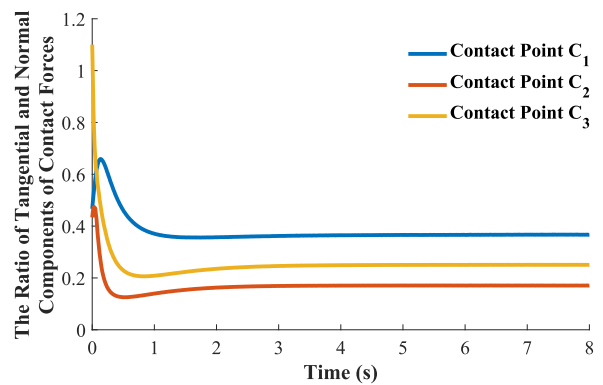**FIGURE 24.** The contact force in contact point 3.

FIGURE 25. The ratio of tangential and normal components of the contact forces.

for the current actuator. Under those driving joint torques, the angular displacements and the angular velocities of finger joints are given in Fig. 14- Fig. 19, which are continuous and convergent. For the contact points on the surface of the object, the angular displacement and velocity of local parameters $\alpha_{oi}(i=1,2,3)$ are shown in Fig. 20- Fig. 21. There is a small displacement of each contact point related to the surface of the object with a low velocity, which close to 0 in 3s.

According to Theorem 3, the fingertip contact forces F_{xi}^c of the ith finger can be calculated and represented by two components as $\{F_{it}, F_{in}\}^T$ in the work space. The simulation results of F_{xi}^c are given in Fig. 22- Fig. 24. Besides, the ratio of tangential and normal components of F_{xi}^c shown in Fig. 25 are all less than 1.2, which means those contact forces could be applicable when the coefficient of the friction that the material of the fingertips is larger than 1.2.

TABLE 3. The terminology nomenclature.

Symbol	Definition	Unit
$\{O_B\}$	primary coordinate frame of the three-fingered robotic hand	−
$\{O_{Bi}\}$	i^{th} finger's primary coordinate frame	−
$\{O_{i(j-1)}\}$	j^{th} joint coordinate frame of ith finger	−
$\{O_{fi}\}$	fixed coordinate frame in the mass center of the ith fingertip	−
$\{O_o\}$	object coordinate frame located at its mass center	−
C_i	i^{th} contact-point	−
$\{O_{Ci}\}$	fixed coordinate frame at the contact point C_i	−
$\alpha_{fi} \in \mathbf{R}^2$	i^{th} fingertip surface local parameters of ith contact-point	−
$\alpha_{oi} \in \mathbf{R}^2$	object surface local parameters of ith contact-point	−
$q_{fi} \in \mathbf{R}^6$	generalized coordinates of the ith finger ($q_{fi} = [q_{fi_1}, q_{fi_2}, q_{fi_3}, q_{fi_4}, \alpha_{fi}]^T$)	rad
$q_{oi} \in \mathbf{R}^8$	generalized coordinates of the target object regarding the ith contact point ($q_{oi} = [x_o, y_o, z_o, \phi_o, \theta_o, \psi_o, \alpha_{oi}]^T$)	mm or rad
$^{fi}C_{fi}(\cdot) : \mathbf{R}^2 \to \mathbf{R}^3$	mapping from fingertip surface to $\{O_{fi}\}$	−
$^oC_{oi}(\cdot) : \mathbf{R}^2 \to \mathbf{R}^3$	mapping from fingertip surface to $\{O_B\}$	−
$P_{f_{ci}} \in \mathbf{R}^3$	i^{th} fingertip's surface contact-point represented in the primary coordinate frame $\{O_B\}$	−
$P_{o_{ci}} \in \mathbf{R}^3$	i^{th} object surface contact-point represented in the primary coordinate frame $\{O_B\}$	−
$P_{fi} \in \mathbf{R}^3$	position vector of the ith fingertip's mass center	mm
$P_o \in \mathbf{R}^3$	position vector of the target object's mass center	mm
$R_{fi} \in \mathbf{R}^{3\times3}$	rotation matrix of $\{O_{fi}\}$ relative to the primary coordinate frame $\{O_B\}$	−
$R_o \in \mathbf{R}^{3\times3}$	rotation matrix of $\{O_o\}$ relative to the primary coordinate frame $\{O_B\}$	−
$J_{fi} \in \mathbf{R}^{6\times4}$	i^{th} finger's Jacobian matrix mapping from the joint to the fingertip	−
$R_{ci} \in \mathbf{R}^{3\times3}$	rotation matrix of $\{O_{Ci}\}$ relative to the primary coordinate frame $\{O_B\}$	−
FC_i	friction cone at contact-point C_i	−
$G_c \in \mathbf{R}^{6\times12}$	grasp matrix	−
$M_{fi} \in \mathbf{R}^{6\times6}$	the singular inertial matrix of the ith finger subsystem	$kg \cdot mm^2$ or kg
$F_{fi} \in \mathbf{R}^6$	the external force includes the centrifugal/Coriolis force and the gravity force of the ith finger subsystem	$N \cdot m$ or N
$\tau_{fi} \in \mathbf{R}^6$	the control torques applied by the ith finger's joint motors ($\tau_{fi} = [\tau_{i1}, \tau_{i2}, \tau_{i3}, \tau_{i4}, 0, 0]^T$)	$N \cdot m$
$M_o \in \mathbf{R}^{12\times12}$	the singular inertial matrix of the target object	$kg \cdot mm^2$ or kg
$F_o \in \mathbf{R}^{12}$	the external force includes the centrifugal/Coriolis force and the gravity force of the target object	$N \cdot m$ or N
$q_o \in \mathbf{R}^{12}$	re-selected generalized coordinates of the target object ($q_o = [x_o, y_o, z_o, \phi_o, \theta_o, \psi_o, \alpha_{o1}, \alpha_{o2}, \alpha_{o3}]^T$) (a compact version of q_{oi} used in Section VI)	mm or rad
$M \in \mathbf{R}^{30\times30}$	the inertial matrix of the hand-object manipulation system (M=blkdiag$[M_{f1}, M_{f2}, M_{f3}, M_o]$)	$kg \cdot mm^2$ or kg
$\tau_f \in \mathbf{R}^{18}$	the control torques applied by the dexterous robotic hand's joint motors ($\tau_f = [\tau_{f1}^T, \tau_{f2}^T, \tau_{f3}^T]^T$)	$N \cdot m$
$F \in \mathbf{R}^{30}$	the external forces of the hand-object manipulation system ($F = [F_{f1}^T, F_{f2}^T, F_{f3}^T, F_o^T]^T$)	$N \cdot m$ or N
$q \in \mathbf{R}^{30}$	the generalized coordinates of the hand-object manipulation system ($q = [q_{f1}^T, q_{f2}^T, q_{f3}^T, q_o^T]^T$)	mm or rad
$f_{xi}^c \in \mathbf{R}^2$	the ith fingertip contact force ($f_{xi}^c = [f_{it}, f_{in}]^T$)	N

Considering the simulation results mentioned above, with the control design in (80), the dexterous robotic hand under the pure rolling contact constraints can accurately manipulate the target object to track the desired trajectory.

VIII. CONCLUSION AND FUTURE WORK

A novel control framework is proposed for the dexterous robotic hand in pure rolling contact with an object. The dexterous robotic hand and the target object is considered as an entire system for the following analysis. First, the contact constraints under the pure rolling is formulated and derived in the second order form. The freedom degrees of the rolling contact between each finger and the target object is two, which means the rolling contact could generate two independent motions for the object. Second, by using the second order contact constraints, the dynamics modeling of the hand-object manipulation system is constructed by the extended Udwadia-Kalaba equation without the singularity guarantee of the inertia matrix and any auxiliary variables. Based on the dynamic model, the paper derives the fingertip contact forces model in the work space using only the generalized coordinates of the hand-object system. Third, the manipulation task is treated as a constraint-following problem. An integrated manipulation control strategy is proposed in two portions. The contact forces model based feed-forward portion is designed to drive the motion of the target object in the desired trajectory without initial deviation. The feedback control portion is formulated to eliminate the initial error. To enhance the performance of the manipulation control, the grasping planning of the robotic hand is pre-designed to ensure the grasping stability in the manipulation task. Finally, the proposed control strategy's effectiveness is substantiated through a rigorous theoretical analysis. Moreover, a three-fingered robot hand is used to demonstrate the feasibility of the proposed control method.

The proposed control design relies on the precise kinematic and dynamic models of the hand manipulation system. While, obtaining the accurate system models, including the precise modeling parameters, is a significant challenge and time-consuming in the practical applications. To enhance the practicability of the proposed approach, the future work will focus on improving the proposed control to adapt for the simplified system, and be robust to the uncertainty raised by the simplification of the system models.
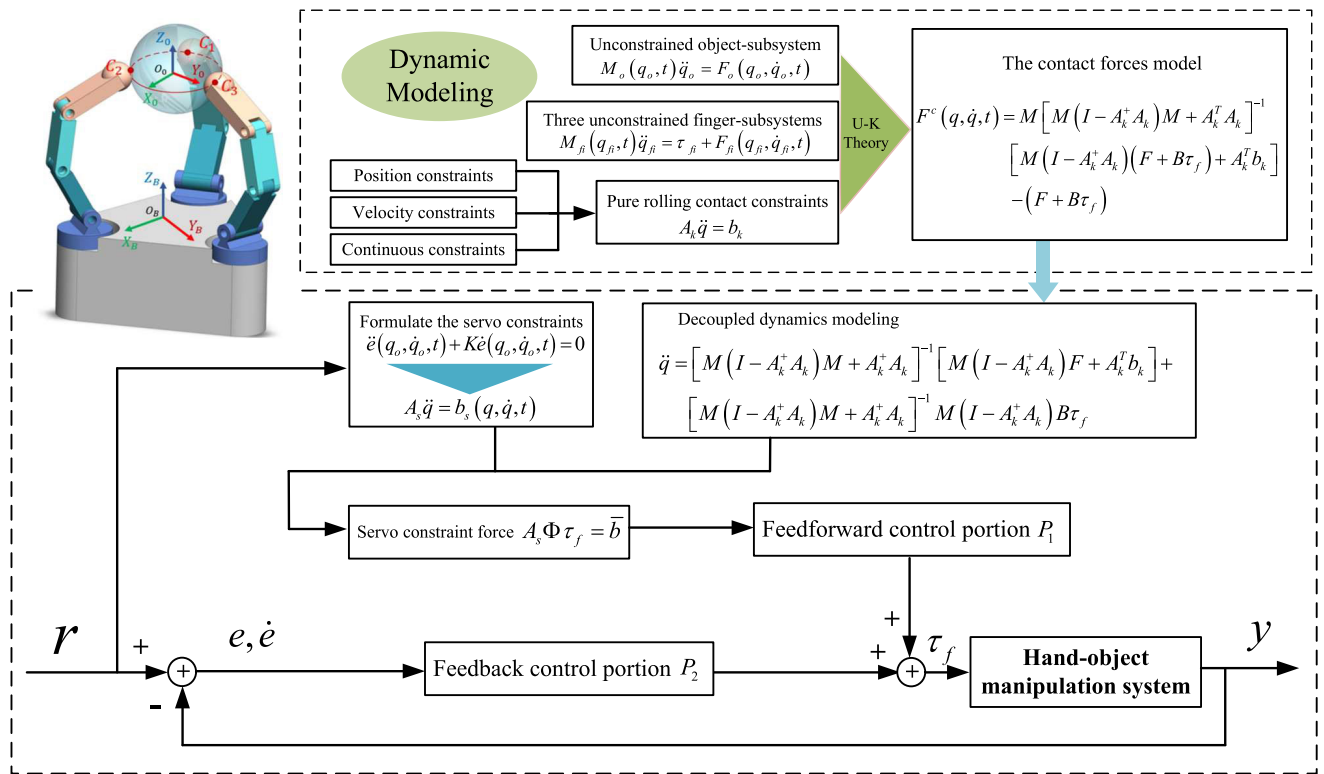
FIGURE 26. The architecture of dynamic modeling and control strategy.

APPENDIX A
THE TERMINOLOGY NOMENCLATURE

This section provides a comprehensive list of nomenclature symbols, units utilized throughout the paper (Table 3).

APPENDIX B
ARCHITECTURE OF DYNAMIC MODELING AND CONTROL STRATEGY

The architecture of dynamic modeling and control strategy is shown in Fig. 26. As the control strategy depicted in Fig. 26, the system's input $r \in R^3$ is the desired position of target object, the system's output $y = q_o = [x_o^d, y_o^d, z_o^d] \in R^3$ is the actual target object's position in the primary coordinate frame $\{O_B\}$. Hence, the servo constraints is formulated in (72) or in matrix form (73). Combined with the decoupled constrained contact force model, the servo constraint force model is constructed in (74), which is the driven force for the target object to follow the desired position r (q_o^d) and used to design the feed-forward control p_1 in (81). Meanwhile, the feedback control p_2 in (82) is designed to eliminate the initial positional errors. Finally, the total control torque applied to the manipulation system is given by $\tau_f = p_1 + p_2$.

REFERENCES

[1] H. Yang, G. Wei, L. Ren, Z. Qian, K. Wang, H. Xiu, and W. Liang, "An affordable linkage-and-tendon hybrid-driven anthropomorphic robotic hand—MCR-hand II," *J. Mech. Robot.*, vol. 13, no. 2, Apr. 2021, Art. no. 024502.

[2] X. Jin, Y. Fang, D. Zhang, and J. Gong, "Design of dexterous hands based on parallel finger structures," *Mechanism Mach. Theory*, vol. 152, Oct. 2020, Art. no. 103952.

[3] U. Kim, D. Jung, H. Jeong, J. Park, H.-M. Jung, J. Cheong, H. R. Choi, H. Do, and C. Park, "Integrated linkage-driven dexterous anthropomorphic robotic hand," *Nature Commun.*, vol. 12, no. 1, pp. 1–13, Dec. 2021.

[4] X. Jin, Y. Fang, D. Zhang, and H. Zhang, "Synthesis of 3-[P][S] parallel mechanism-inspired multimode dexterous hands with parallel finger structure," *J. Mech. Design*, vol. 142, no. 8, Aug. 2020, Art. no. 083301.

[5] M. V. Liarokapis, P. K. Artemiadis, and K. J. Kyriakopoulos, "Telemanipulation with the DLR/HIT II robot hand using a dataglove and a low cost force feedback device," in *Proc. 21st Medit. Conf. Control Autom.*, Jun. 2013, pp. 431–436.

[6] H. Liu, B. Zhao, Z. Liu, and K. Xu, "Design of a lightweight single-actuator multi-grasp prosthetic hand with force magnification," *J. Mech. Robot.*, vol. 12, no. 5, Oct. 2020, Art. no. 051014.

[7] M. Controzzi, F. Clemente, D. Barone, A. Ghionzoli, and C. Cipriani, "The SSSA-MyHand: A dexterous lightweight myoelectric hand prosthesis," *IEEE Trans. Neural Syst. Rehabil. Eng.*, vol. 25, no. 5, pp. 459–468, May 2017.

[8] H. Kawasaki and T. Mouri, "Humanoid robot hand and its applied research," *J. Robot. Mechatronics*, vol. 31, no. 1, pp. 16–26, Feb. 2019.

[9] Z. Deng, Y. Jonetzko, L. Zhang, and J. Zhang, "Grasping force control of multi-fingered robotic hands through tactile sensing for object stabilization," *Sensors*, vol. 20, no. 4, p. 1050, Feb. 2020.

[10] K. Kawaharazuka, K. Tsuzuki, M. Onitsuka, Y. Asano, K. Okada, K. Kawasaki, and M. Inaba, "Object recognition, dynamic contact simulation, detection, and control of the flexible musculoskeletal hand using a recurrent neural network with parametric bias," *IEEE Robot. Autom. Lett.*, vol. 5, no. 3, pp. 4580–4587, Jul. 2020.

[11] L. Cui, J. Sun, and J. S. Dai, "In-hand forward and inverse kinematics with rolling contact," *Robotica*, vol. 35, no. 12, pp. 2381–2399, Dec. 2017.

[12] J. Shi, J. Z. Woodruff, P. B. Umbanhowar, and K. M. Lynch, "Dynamic in-hand sliding manipulation," *IEEE Trans. Robot.*, vol. 33, no. 4, pp. 778–795, Aug. 2017.

[13] H. Deng, G. Zhong, X. Li, and W. Nie, "Slippage and deformation preventive control of bionic prosthetic hands," *IEEE/ASME Trans. Mechatronics*, vol. 22, no. 2, pp. 888–897, Apr. 2017.

[14] T. Yoshikawa, "Multifingered robot hands: Control for grasping and manipulation," *Annu. Rev. Control*, vol. 34, no. 2, pp. 199–208, Dec. 2010.

[15] T. Li, K. Srinivasan, M. Q. Meng, W. Yuan, and J. Bohg, "Learning hierarchical control for robust in-hand manipulation," in *Proc. IEEE Int. Conf. Robot. Autom. (ICRA)*, May 2020, pp. 8855–8862.

[16] Y. Yokokohji, J. S. Martin, and M. Fujiwara, "Dynamic manipulability of multifingered grasping," *IEEE Trans. Robot.*, vol. 25, no. 4, pp. 947–954, Aug. 2009.

[17] R. Zhao, J. Yu, H. Yang, and Y.-H. Chen, "Contact constraints-based dynamic manipulation control of the multi-fingered hand robot: A force sensorless approach," *Nonlinear Dyn.*, vol. 107, no. 1, pp. 1081–1105, Jan. 2022.

[18] J. Xu, F. Zeng, Y.-H. Chen, and H. Guo, "Robust constraint following stabilization for mechanical manipulators containing uncertainty: An adaptive φ approach," *IEEE Access*, vol. 6, pp. 58728–58736, 2018.

[19] R. Zhao, L. Wu, and Y.-H. Chen, "Robust control for nonlinear delta parallel robot with uncertainty: An online estimation approach," *IEEE Access*, vol. 8, pp. 97604–97617, 2020.

[20] C. Li, Y.-H. Chen, H. Sun, and H. Zhao, "Optimal design of high-order control for fuzzy dynamical systems based on the cooperative game theory," *IEEE Trans. Cybern.*, vol. 52, no. 1, pp. 423–432, Jan. 2022.

[21] C.-H. Xiong, W.-R. Chen, B.-Y. Sun, M.-J. Liu, S.-G. Yue, and W.-B. Chen, "Design and implementation of an anthropomorphic hand for replicating human grasping functions," *IEEE Trans. Robot.*, vol. 32, no. 3, pp. 652–671, Jun. 2016.

[22] F. E. Udwadia and P. Phohomsiri, "Explicit equations of motion for constrained mechanical systems with singular mass matrices and applications to multi-body dynamics," *Proc. Roy. Soc. A, Math., Phys. Eng. Sci.*, vol. 462, no. 2071, pp. 2097–2117, Jul. 2006.

[23] Y.-H. Chen, "Constraint-following servo control design for mechanical systems," *J. Vib. Control*, vol. 15, no. 3, pp. 369–389, Mar. 2009.

[24] R. Zhao, M. Li, Q. Niu, and Y.-H. Chen, "Udwadia–Kalaba constraint-based tracking control for artificial swarm mechanical systems: Dynamic approach," *Nonlinear Dyn.*, vol. 100, no. 3, pp. 2381–2399, May 2020.

[25] F. E. Udwadia and R. E. Kalaba, "Explicit equations of motion for mechanical systems with nonideal constraints," *J. Appl. Mech.*, vol. 68, no. 3, pp. 462–467, May 2001.

[26] F. E. Udwadia, "On constrained motion," *Appl. Math. Comput.*, vol. 164, no. 2, pp. 313–320, 2005.

[27] M. A. Murray-Lasso, "Alternative methods of calculation of the pseudo inverse of a non full-rank matrix," *J. Appl. Res. Technol.*, vol. 6, no. 3, pp. 170–183, Dec. 2008.

[28] M. A. Rakha, "On the Moore–Penrose generalized inverse matrix," *Appl. Math. Comput.*, vol. 158, no. 1, pp. 185–200, 2004.

[29] R. Rosenberg, *Analytical Dynamics*. Berlin, Germany: Springer, 1977.

[30] H. V. Henderson and S. R. Searle, "On deriving the inverse of a sum of matrices," *SIAM Rev.*, vol. 23, no. 1, pp. 53–60, Jan. 1981.

[31] A. Cole, J. Hauser, and S. Sastry, "Kinematics and control of multifingered hands with rolling contact," in *Proc. IEEE Int. Conf. Robot. Autom.*, Apr. 1988, pp. 228–233.

[32] J. Huang, Y. H. Chen, and K. Guo, "Novel approach to multibody system modeling: Cascading and clustering," *J. Aerosp. Eng.*, vol. 27, no. 2, pp. 279–290, Mar. 2014.

[33] R. Yu, Y.-H. Chen, H. Zhao, and H. Sun, "Uniform ultimate boundedness for underactuated mechanical systems as mismatched uncertainty disappeared," *Nonlinear Dyn.*, vol. 95, no. 4, pp. 2765–2782, Mar. 2019.

[34] J.-J. E. Slotine and W. Li, *Applied Nonlinear Control*, vol. 199. Englewood Cliffs, NJ, USA: Prentice-Hall, 1991.

[35] A. Caldas, M. Grossard, M. Makarov, and P. Rodriguez-Ayerbe, "Task-level dexterous manipulation with multifingered hand under modeling uncertainties," *J. Dyn. Syst., Meas., Control*, vol. 144, no. 3, pp. 31001–31012, Mar. 2022.

SHUWEI ZHAO received the B.S. degree in mechanical engineering from Chang'an University, China, in 2021, where he is currently pursuing the master's degree in mechanical engineering. His research interests include dynamic systems and robot intelligent control.

JIN YU received the B.S. and M.S. degrees in mechanical engineering from Chang'an University, in 2019 and 2022, respectively. She is currently pursuing the Ph.D. degree in control science and engineering with the School of Automation, Beijing Institute of Technology, Beijing, China. Her research interests include the structural design and control algorithms of intelligent prosthetics.

YE-HWA CHEN received the Ph.D. degree from the University of California at Berkeley, Berkeley, CA, USA, in 1985. He is currently a Professor with The George W. Woodruff School of Mechanical Engineering, Georgia Institute of Technology. His research interests include fuzzy dynamical systems, fuzzy reasoning, and modeling and control of mechanical systems. He received the IEEE TRANSACTIONS ON FUZZY SYSTEMS Outstanding Paper Award from the IEEE Neural Networks Council, in 2001. He has been serving as a regional editor and/or an associate editor for six journals.

RUIYING ZHAO (Member, IEEE) received the Ph.D. degree, in 2015. She visited The George W. Woodruff School of Mechanical Engineering, Georgia Institute of Technology, Atlanta, GA, USA, as a Visiting Ph.D. Student, from September 2012 to September 2014. She is currently an Associate Professor with Chang'an University, China. Her research interests include multi-body system dynamics, robust control of mechanical systems, fuzzy dynamical systems, robot intelligent control, and energy-saving control for construction machinery.

• • •